*Article*

# The Morphodynamics of a Double-Crescent Bar System under a Mediterranean Wave Climate: Leucate Beach

Pierre Feyssat *, Raphaël Certain, Nicolas Robin, Olivier Raynal, Antoine Lamy, Jean-Paul Barusseau and Bertil Hebert

CEFREM, UMR CNRS 5110, Université de Perpignan Via-Domitia, 66100 Perpignan, France
* Correspondence: pierre.feyssat@univ-perp.fr

**Abstract:** The morphodynamics of the Leucate double-crescent bar system was studied over twenty years using bathymetric data supplemented by satellite images and video monitoring. Eleven different bar typologies were identified, mostly based on existing beach state classifications (Low-Tide Terrace, Transverse Bar and Rip, Rhythmic Bar and Beach), also including new heterogeneous typologies (TBR/LTT, RBB HP/RBB, TBR/RBB). The inner bar shows greater variability, with 10 different typologies observed, while the outer bar shows only three different typologies. Summer low-energy periods are dominated by TBR/LTT and TBR typologies, while RBB, although common throughout the year, dominates winter periods along with disrupted bar configurations. The return to less energetic periods in spring is associated with the establishment of heterogeneous typologies. The outer bar has a fairly stable position, although breaches at the embayments and slight movements of its horns can occur following particularly energetic episodes. The inner bar, on the other hand, is much more dynamic, with more common breaches at the embayments and significant cross-shore movement of the horns. Seasonal changes in bar typology do not lead to bar renewal through destruction/reconstruction. Overall, the morphological and typological characteristics of the bar system described here seem somewhat unique compared to the existing literature.

**Keywords:** nearshore bars; double-crescent bar; morphological coupling; Mediterranean Sea; Gulf of Lions

## 1. Introduction

Sandy beaches on wave-dominated coasts often feature nearshore bars [1]. These bars serve as preferential points of wave energy dissipation by surf breaking [2], and thus provide a primary form of beach protection, which has important implications for both short- and long-term coastal mobility [3,4].

Three main beach states have been identified in relation to environmental parameters: dissipative, intermediate and reflective [5]. Intermediate beaches have been divided into four sub-states ranked in order of decreasing energy supplied to the system and according to the resulting morphologies: Longshore Bar and Trough (LBT), Rhythmic Bar and Beach (RBB), Transverse Bar and Rip (TBR) and Low-Tide Terrace (LTT) [2,5–7]. These classifications have subsequently been supplemented by specific studies on various environments—e.g., refs. [8–15]. However, these classifications represent a static and idealized view of nature, and we require a better understanding of the processes and controlling factors associated with morphological changes within intermediate beach state transitions [8].

Typology transitions are most often attributed to the quantities of energy delivered to the bar system [5,7,16], expressed either in terms of significant wave height (Hs), wave energy (P) or a dimensionless number (Ω). These transitions in beach state can also be attributed to wave incidence [17–19]. These studies generally focus on beaches characterized by a large tidal range (>1 m) and a high-energy wave climate—e.g., refs. [17,20,21].

There are fewer studies of crescentic bars in low-energy environments with a small tidal range (such as in the Mediterranean Sea), but we can cite the following studies that provide an overview of sandbar dynamics in the Mediterranean: Spain [22,23], France [12,13], Israel [24] and Italy [25–27]. It is essential to acquire some knowledge of beach dynamics in varied and contrasting environments to get insight into physical mechanisms driving bar transitions, thus enabling effective management strategies and improving the assessment of sandbar resilience [28,29].

Various conceptual models have been proposed to describe the morphology and behavior of nearshore bars on a seasonal to multi-annual scale [30]. The Net Offshore Migration (NOM) model is commonly observed and recognized, particularly in the case of straight bars. It describes the creation, offshore migration and degeneration of nearshore bars, which can take years or even decades [27,31–36]. Certain authors suggest that the NOM model can also be applied to slightly crescentic bars [23]. The Oscillation around a Point of Equilibrium (OPE) model for crescentic bars implies that a bar oscillates around a long-term equilibrium position under the constraint of a diverse energy spectrum [37]. So far, only a few studies have been carried out on Mediterranean crescentic bars, which are characterized by low tidal amplitudes—e.g., refs. [23,25,27,37]. The low agitation that characterizes these environments makes direct bathymetry measurements (e.g., single or multi-beam echo sounder) relatively straightforward [38].

Regarding the specific dynamics of crescentic bars (RBB) on an event scale, numerical models can satisfactorily reproduce field observations. For example, models can simulate the formation of crescentic bars for shore normal waves—e.g., refs. [39–44], and their linearization during periods of oblique incidence waves [17,20,45,46]. Models also predict that the formation of crescentic bars is strongly linked to the underlying bathymetry [47–50]. However, model predictions are not always consistent with field observations, and model validation is generally difficult due to the lack of appropriate field data [51]. Although the results of such studies can be very revealing, they are most often limited to single-bar systems with very energetic forcing conditions, both for models—e.g., refs. [52–56], and for observations [3,51,57]. Few studies address the case of RBB double-bar systems in Mediterranean-type environments (low tidal range, long periods of good weather, short intense storms).

In double-bar systems, seaward bars are characterized by a greater amplitude of crescents [58] with the inner and outer bars evolving on different spatiotemporal scales [8]. The outer bar tends to be inactive, and when a crescentic form has developed, it can persist for long periods (up to months) [10,21,59]. The inner bar tends to be less regularly spaced and more active than the outer bar, as the horns may connect with the coastline. In a system with multiple nearshore bars, it is also possible to observe coupling mechanisms between two distinct bars, or between crescentic bars and beach megacusps [6,11,23,60–62]. The height and angle of incidence of offshore waves, as well as the morphology of the outer bar, strongly influence the coupling between bars [8,11,60,61,63,64]. Out-of-phase coupling (the horns face each other) develops during periods of small waves perpendicular to the coast [23,54,65,66], favoring a two-cell hydrodynamic circulation. In-phase coupling (patterns are expressed in parallel) develops with medium-intensity waves perpendicular to the coast, favoring a single-cell circulation [23,54,65,66]. Finally, downwave coupling (lateral offset between bar horns and embayments) is the result of meandering currents (flowing on either side of the bar longshore) created by moderately energetic but highly oblique waves [23,62].

The full dynamics of rhythmic sandbars in nature are far from being understood due to many factors interacting. To get insight into this issue, observational studies in as many different types of beaches as possible are highly valuable. The aim of this study is to describe the general functioning and changes in the typology of a double-crescent bar system at the Leucate site evolving in a Mediterranean regime, based on 20 years of observations (from 2000 to 2020) mainly based on accurate bathymetric surveys. We also set out in particular (1) to define the typologies of the inner and outer bar system; (2) to

observe their representativeness over the 20 years of observations and identify a seasonality; (3) to describe the event dynamics of the bar system and the transitions from one typology to another, with the aim of identifying the controlling parameters; (4) to characterize the coupling relationships in the bar system; and, finally, (5) to suggest a conceptual model voluntarily, mainly based on morphological evolution observed for this Mediterranean bar system, and confront it with the general classification already established. The latter will enable us to determine the specificity of the Mediterranean regime.
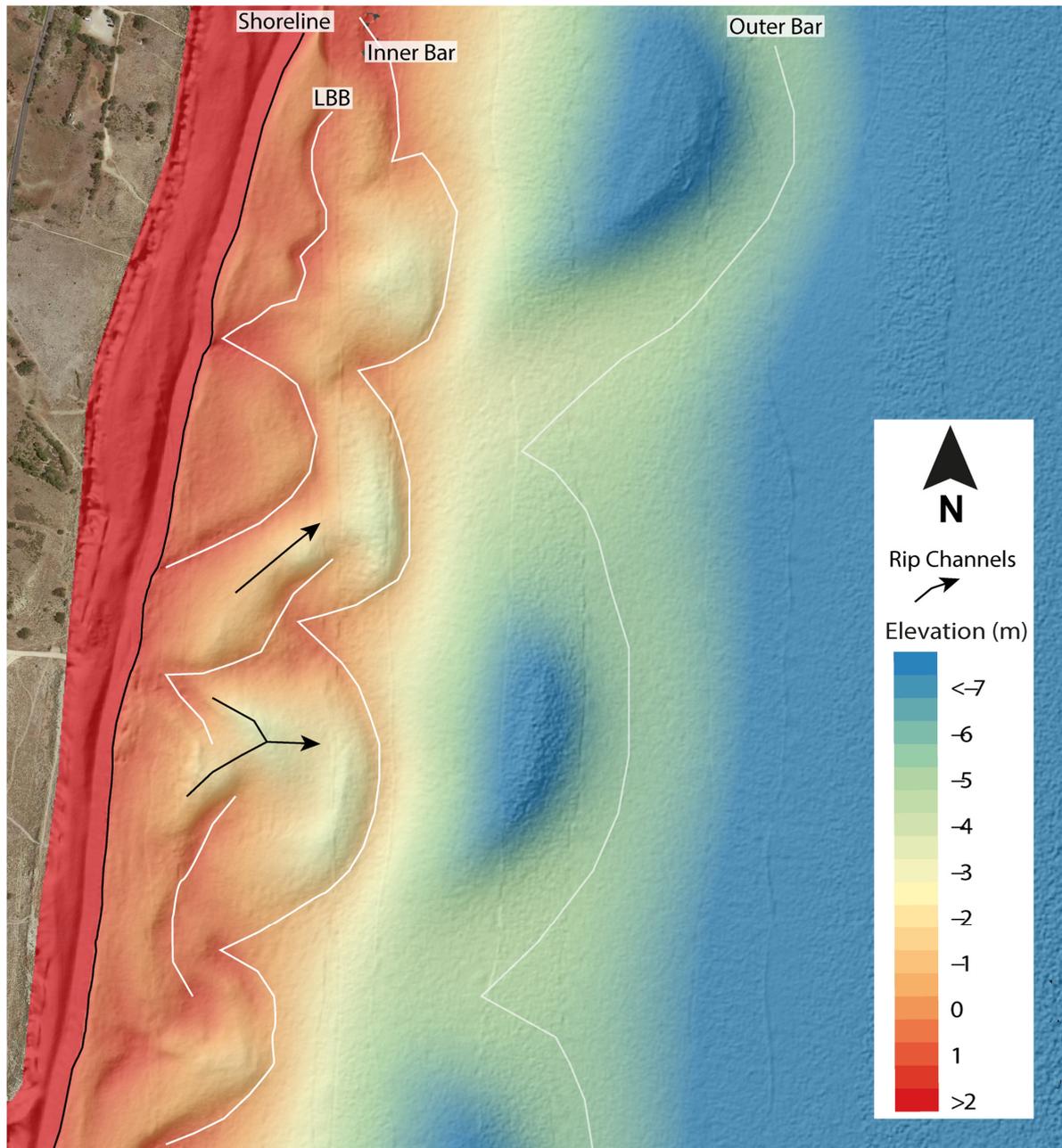
## 2. Study Site

The study site is located in the southern part of the Gulf of Lions, along the French coast of the Mediterranean Sea (Figure 1a,b). The mean tidal range is around 0.3 m, which is among the smallest amplitudes observed in microtidal environments. The Mediterranean climate is characterized by long periods of fair weather, interrupted by short periods of storms, which can be violent. Offshore-directed winds predominate at Leucate [67,68] (blowing 73% of the time, Figure 1c), generating offshore-directed waves that do not impact the study site (grey area on the wave rose, Figure 1d). The onshore wind is less frequent (blowing 27% of the time) and is accompanied by S/SE waves; it is associated with strong winter storms of short duration [69]. The onshore-directed waves are characterized by greater heights and longer periods ($5 \leq Ts \leq 10$ s) due to their more extensive fetch [70]. In this present study, a storm is defined as a wave event in which Hs exceeds the 2 m threshold value commonly used in the region [13,71]. According to this definition, at the Leucate site, about seven to eight storm events are reported per year [72]. Hs can reach up to more than 6.5 m during severe storms [72,73]. A certain seasonality can be observed in these forcing regimes: in summer, sea breezes are frequent, while in late autumn, winter and spring, they are characterized by more violent onshore wind events, punctuated by storms induced by sea winds [70].
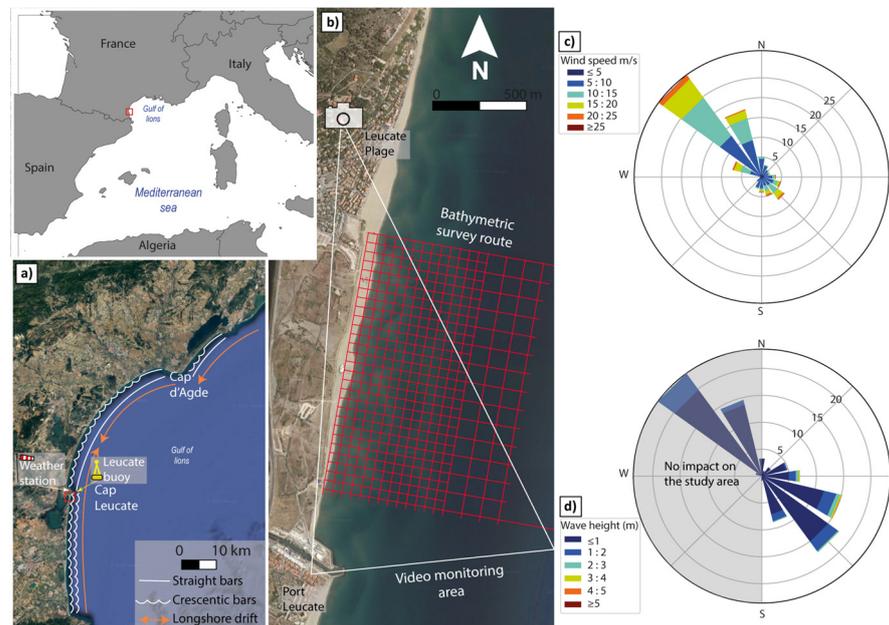


**Figure 1.** Location of the study site (outlined in red). (**a**) Typologies of nearshore bars (in white) in the central and southern parts of the Gulf of Lions (from Aleman et al., 2015 [69]). The resulting annual longshore drift current directions are shown in orange. The study site is outlined in red. (**b**) The study site, Leucate Beach, with bathymetric profile positions in red and video imagery footprint in white. (**c**) Wind conditions (measured at the tip of Cap Leucate, 2.1 miles offshore at a depth of 40 m; see panel a). (**d**) Wave conditions (measured at 40 m depth, about 3.9 km ahead of the weather station; see panel (**a**). Meteorological data are given for the period 2007–2022.

Leucate beach (2.8 km long) is described as intermediate ($\Omega$ = 3.7), with a permanent double-crescent nearshore sandbar system giving an undulating pattern to the shoreline [13,69]. The inner bar is located around 200 m from the shore at a depth of between −1 and −2 m, with a wavelength of around 300 m. The outer bar is located around 600 m from the shore at a depth of around −5.5 m, with a wavelength of around 600 m (Figure 2). The average sediment grain size on the coast is 0.43 mm and the slope is 1.2°.



**Figure 2.** LiDAR topo-bathymetry (Litto3D 2014) of the study site with bar crest lines highlighted in white. LBB: Low Beach Bars.

The configuration of the double-bar system refracts and attenuates waves, particularly as they pass over the outer bar [5,42,52,74]. Similar systems of double crescentic bars are found throughout the southern sector of the Gulf of Lions, which covers 40.5 km of coastline (Figure 1a). In the central sector, which covers 67 km of coastline, only the inner bar is crescentic, with the outer bar being linear [13]. In some parts of the southern and central

sectors of the Gulf of Lions, one horn of the inner bar is less developed and is located further offshore [13], leaving a larger accommodation space between the bar and the shoreline (Figure 2), allowing for the growth of a third proximal bar system known as a Low Beach Bar (LBB) [12,13,75]. The LBB is very reactive to changes in hydrodynamic conditions due to their positions in the very shallow water and responds along an increasing morphological continuum from sandy plateaus to RBB and disrupted RBB if the energy level increases. The LBB is distinct from other transitory proximal systems observed in the literature due to its resilience over several years and lack of offshore migration to replace the inner bar. It does, however, appear to be able to merge and exchange sediments with the beach face [75].

## 3. Materials and Methods

### 3.1. Morphology of the Nearshore

The methodology is primarily based on the analysis of event-driven bathymetric data (39 surveys). Once the main typologies have been identified, this analysis is extended and completed by the use of satellite images (40 images). Twice a year (between 2000 and 2020), before and after the winter season, the morphology and typology of the bars are visually assessed on satellite images. Lastly, a video monitoring campaign was carried out to track the dynamics of the bar system during storm events. This methodology has enabled continuous monitoring of the bar system at the study site over the past 20 years.

#### 3.1.1. Bathymetric Survey

Several instruments have been used over the years for bathymetric surveys. First, a Tritech ST500 single-beam echo sounder was used (TriTech, San Diego, CA, USA), coupled to a DSNP NR51 GNSS DGPS receiver. Then, in 2019, a Tritech PA500 echo-sounder was coupled to an Ashtech Proflex 500/800 (Ashtech, Mumbai, India) or a Trimble R8s DGPS receiver (Westminster, CO, USA). Bathymetric surveys were carried out with a small vessel, using Hypack 2012 software for survey design, data collection and post-processing, with data then being processed on Qgis 3.16. The area from the coastline to 600 m offshore, where the crescentic bars are located, was surveyed with a 50 m × 50 m grid. A second zone extending between 600 m and 900 m from the coast was surveyed with a 100 m × 100 m grid. Z-accuracy is +/− 0.1 m for a single survey and +/− 0.15 m for differential DTMs. The bathymetric approach is easy to implement here, due to the long periods of fair weather between storms. The survey is event-based, with measurements taken before and after morphogenetic periods (i.e., wave episodes Hs > 2 m). A total of 39 digital elevation models (DEM) were used for this study (for survey dates, see Figure 6a), divided into two high-frequency monitoring periods, between March 2006 and January 2009, and a second period between July 2019 and July 2020. All levels expressed in this study are in NGF meters, the official French topographic reference: Lambert 93/RGF93.

#### 3.1.2. Remote Sensing Data

Satellite images were acquired using the open-source CoastSat toolkit [76]. This allows the user to obtain public satellite data (Landsat 5,7,8,9 and Sentinel-2) by exploiting the capabilities of the Google Earth Engine. For each defined region of interest, the resulting images are pre-processed to remove cloudy pixels and improve spatial resolution. Once the images have been downloaded (periods of calm weather with clear water and no surf), the morphological characteristics of the bars (i.e., bar crest position) are digitized manually and measured in Qgis 3.16. The resolution of the digitized ridge positions is estimated at around 10 to 12 m (similar to the shoreline positions detected by the tool, Vos et al., 2019 [76]). Between January 2000 and December 2020, two images per year were processed, in late summer and late winter (40 images processed over the period; see Figure 6a for survey dates). This allows coverage of the most energetic and morphogenic period of the year.

Video monitoring of bar positions took place from 22 March 2020 to 24 April 2020 during periods of marine storms, leading to the acquisition of 17 images (see Figure 6a for

survey periods). A high-resolution digital camera was positioned at a fixed lookout point on the Leucate cliffs (around 40 m above the study area). A series of images was taken using 10–20 min exposures with one shot per second. The images were then averaged (using ImageMagick), corrected for lens distortion (using DxO View Point), the horizon leveled (using XnView), the image registered to allow for superposition (using Gimp) and finally reframed on the study site (using XnView). The images were then georectified using Qgis 3.16, and the positions of shorelines and bar crests were manually picked. The resolution of digitized ridge positions is estimated at around 7 to 10 m.

### 3.1.3. Classification of Bar Typologies

The following conceptual model was proposed for the typology of bar systems, based on observations made using 2009 LiDAR data in the Gulf of Lions [13]. While this model complements the terminologies proposed in the literature (TBR, RBB, LBT, LTT) [2,5,6], certain characteristics have been added to give a more precise and specific description of the Mediterranean regime. This nomenclature is used to identify the different bar typologies observed during this present survey. The RBB typology (Figure 3a) includes configurations with high points (see also Figure 2) where the bar horn is outlined by a wide depocenter and normal configurations where the horn and embayment have the same width. The TBR typology (Figure 3b) is characterized by crescent-shaped bars connected to the coastline by an elongated depocenter giving a transverse bar that can be either normal to the coast or oblique. A crescent usually has two identical horns, but a heterogeneous state is also possible (Figure 3c) when one of the horns is connected to the coast or the preceding bar, but not the other horn (TBR/RBB). Depending on their orientation with respect to the coast, crescents can be oblique or normal (regular), and their embayments may be either uninterrupted or disrupted by rip channel incisions [12]. Finally, a hybrid TBR/LTT state (Figure 3d) has long seaward-curving sandbanks connected to the beach [12].
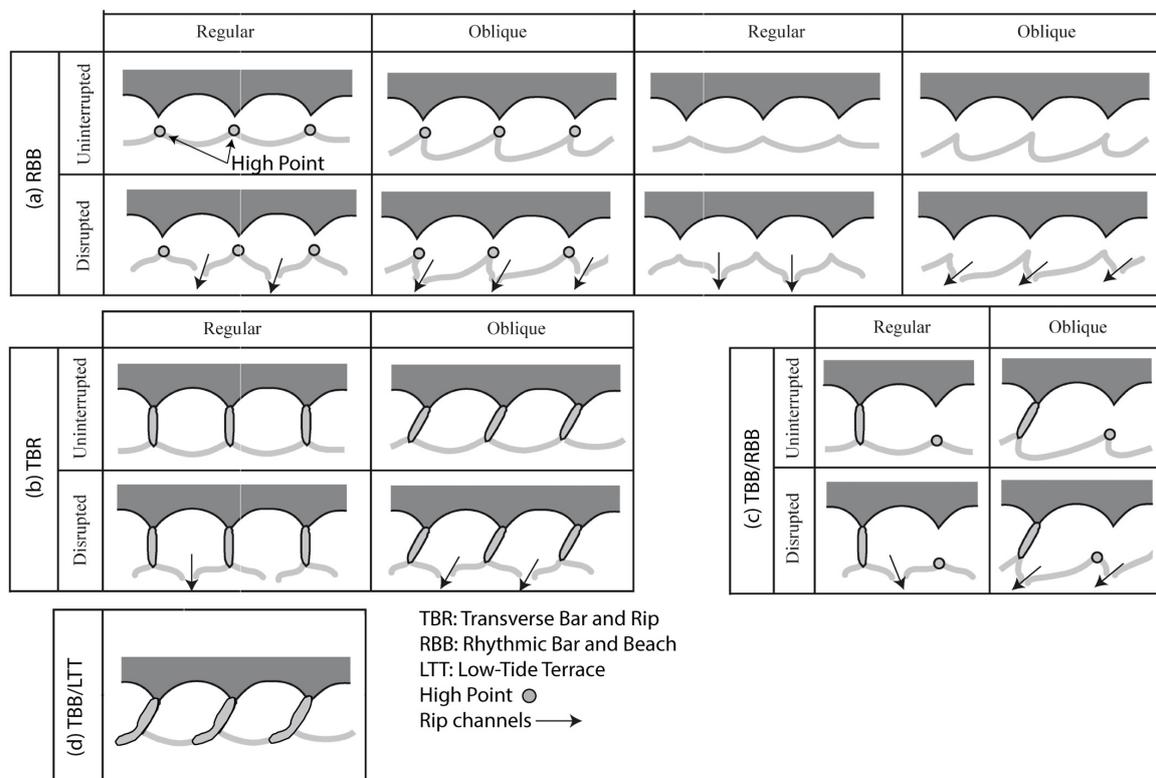


**Figure 3.** Classification of bar typologies observed in the Gulf of Lions, France (after Aleman et al., 2011 [13], modified from Wright and Short, 1984 [5], and Ferrer et al., 2009 [12]). This classification is applied to the inner and outer bars.

In the results section, we classify the bars observed at the study site according to the typologies described in Figure 3. The system is classified as disrupted if there is at least one bar breach in the observation zone.

### 3.1.4. Classification of Bar Coupling Types

The classification of coupling typologies between the two nearshore bars of the system is based on the typology used by de Swart et al., 2022, on a geographically close Mediterranean site [23]. Three types of coupling are possible: in-phase, where bar patterns are expressed in parallel; out-of-phase, where bar horns face each other; and downwave, where there is a lateral offset between bar horns and embayments.

### 3.2. Hydrodynamic and Meteorological Forcing

Morphological and typological evolutions will then be compared with offshore forcing conditions in the following sections (see Sections 4.3–4.5).

Offshore wave conditions are given for the Leucate buoy (moored around 4 km from the study area at a depth of 40 m) using modeling data from the Puerto del Estado website, publicly accessible at the following address: (https://www.puertos.es/; accessed on 4 November 2023).

The wave energy density $E$ (in J/m$^2$) is calculated according to the linear wave theory (1), where $H_{m0}$ is the spectral significant wave height:

$$E = \frac{1}{8}\rho g H_{m0}^2$$

(1)

## 4. Results

### 4.1. Nearshore Typologies Based on 20 Years of Observations

Figure 4 illustrates the 11 different typologies of bars observed during bathymetric surveys at the Leucate site. Figure 5 shows the percentages of occurrence for each typology from LTT to RBB, distinguishing between interrupted and disrupted patterns.

Only three typologies are observed on the outer bar, all of them belonging to the RBB beach state (Figure 5), most often RBB HP Regular (Figure 4a,e–h) (54%) and RRB Regular (Figure 4c,i) (41%), while the RBB Disrupted state accounts for 5% of occurrences (Figure 4b,d,j).

The inner bar displayed a wide variety of typologies (10) during the monitoring period, with RBB (Disrupted, Figure 4c; HP Oblique Disrupted, Figure 4b; Disrupted Regular, Figure 4c) being the most common (51%, Figure 5) and RBB HP Regular being the dominant state (34%). There are no regular TBRs, only oblique TBRs (7%, Figure 4d) and oblique disrupted TBRs (10%, Figure 4e), the latter representing the only case where the disrupted pattern is more common than the corresponding uninterrupted morphology (Figure 5). The TBR/LTT typology (Figure 4j) is poorly represented, with only 7% of observed states. Finally, the most complex cases correspond to heterogeneous states accounting for 25% of observations.

1.  RBB HP/RBB (Figure 5) is the most common case (15% of observations), including 5% that are disrupted (Figure 4f);
2.  TBR/RBB (Figure 4h,i) in our case corresponds to oblique TBRs (which show an elongated depocenter connected to the coastline), with one of the horns not connected to the coastline, which therefore do not develop an RBB configuration (10% of observations, Figure 5).

There is a certain homogeneity in the bar system, with a dominance of RBB typologies (accounting for 51% of cases in the inner bar and 100% in the outer bar; Figure 5), while other states are nevertheless represented over time. In addition, the embayments of the crescents often show persistent channeled incisions following storm events (Figure 4).
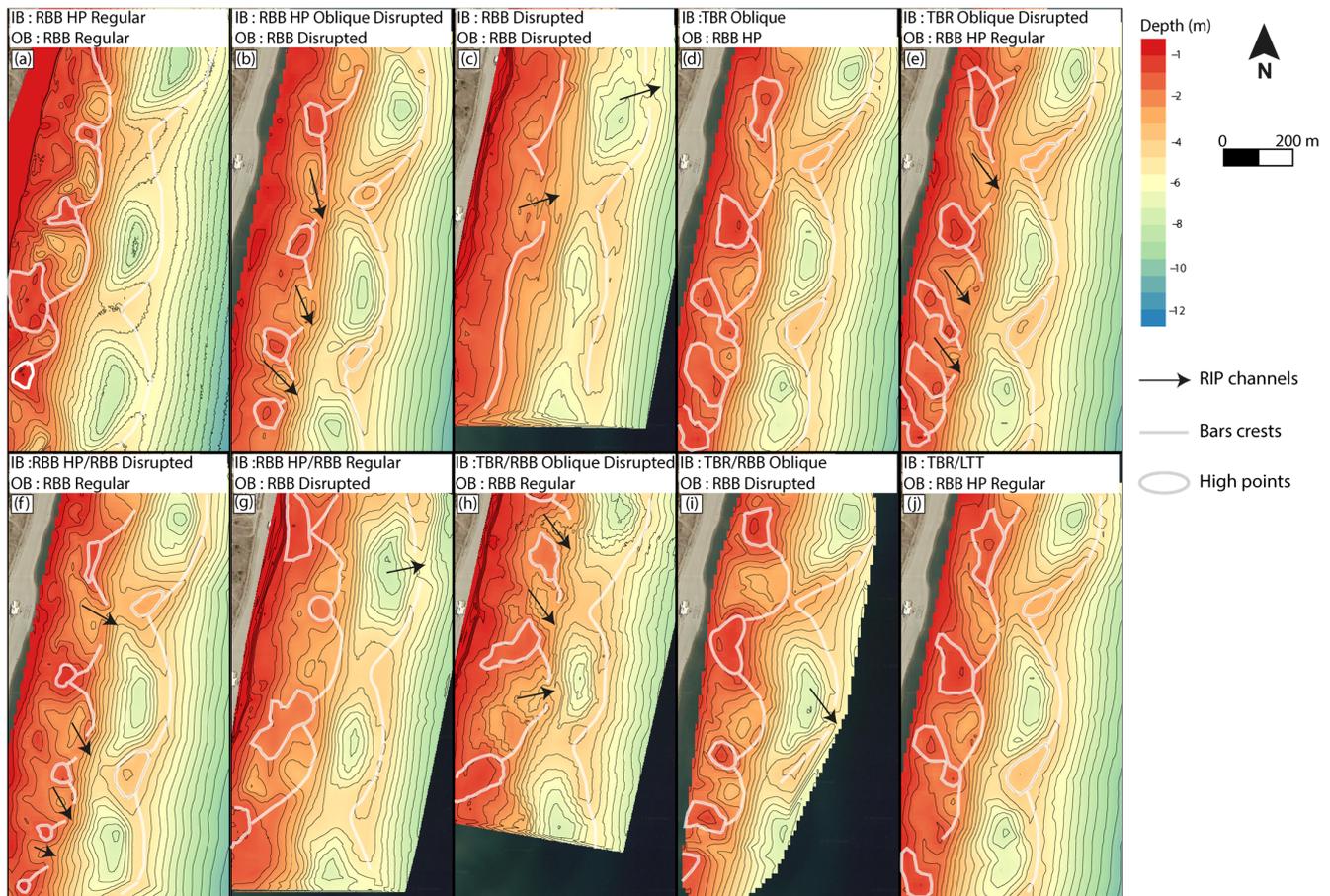
**Figure 4.** Examples of different types of bars observed at the study site (**a**–**j**), taken from bathymetric surveys. See Figure 5 for classification and occurrence.
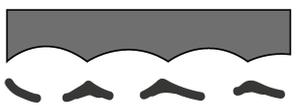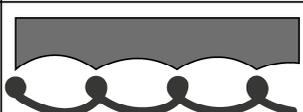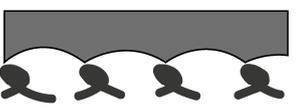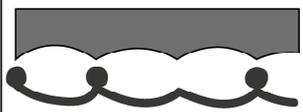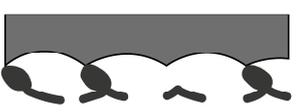
### 4.2. Temporal Evolutions of Bar Typologies on a Seasonal Scale

Wave measurement statistics show two distinct periods (Figures 6 and 7): a summer period (July to September) marked by waves of rather low significant height (Hs < 1 m and Hmax < 1.5 m) (Figure 7a) with short periods (between 2 and 4 s) (Figure 6c) and no storm episodes (Hs > 2 m) (Figure 6a). During winter, the significant mean wave heights are rather high (Hs around 1 m and Hmax > 1.5 m, Figure 7a). During this period, storms can occur with Hs close to 5 m (Figure 6a), and waves show periods of the order of 6 to 8 s (Figure 6b), resulting in wave energy flux of more than 10 kJ/m$^2$ during storm events (Figure 6c).

RBB Regular typologies with or without high points are the most common states observed throughout the year on the outer bar (Figures 6g and 7b). During the most energetic months, RBB Disrupted states (Figure 7b) may be observed, whose existence seems to be linked to particularly energetic episodes (Figure 6c), although it is not possible to determine the effect of wave direction on the development of such typologies.

Inner-bar morphologies, although highly diversified, are dominated by RBB typologies, regardless of the season (Figures 6g and 7c). It is possible, however, to notice a certain seasonality in some observed typologies. RBBs are never disrupted at the beginning of summer (Figure 7c), while Disrupted RBBs are mainly observed during the most energetic months of winter and autumn (Figure 7c), particularly following storm events (Figure 6). TBR variants are observed between April and September (Figure 7c), corresponding to periods of decreasing energy (April to July) and summer calms (July to September) (Figure 7a). Heterogeneous typologies (TBR/RBB and RBB HP/RBB) are observed outside the summer period (Figure 7c); i.e., they are associated with moderately energetic forcing regimes,

essentially between January and April (Figure 7a,c). TBR/LTTs, on the other hand, are mainly observed during less energetic periods, notably in September (Figure 7a,c).



**Figure 5.** Typology of bars observed at Leucate (from 2000 to 2020), based on 79 observations. Gray areas indicate no observations. IB: inner bar; OB: outer bar. The same color code is used for each typology in the following figures.
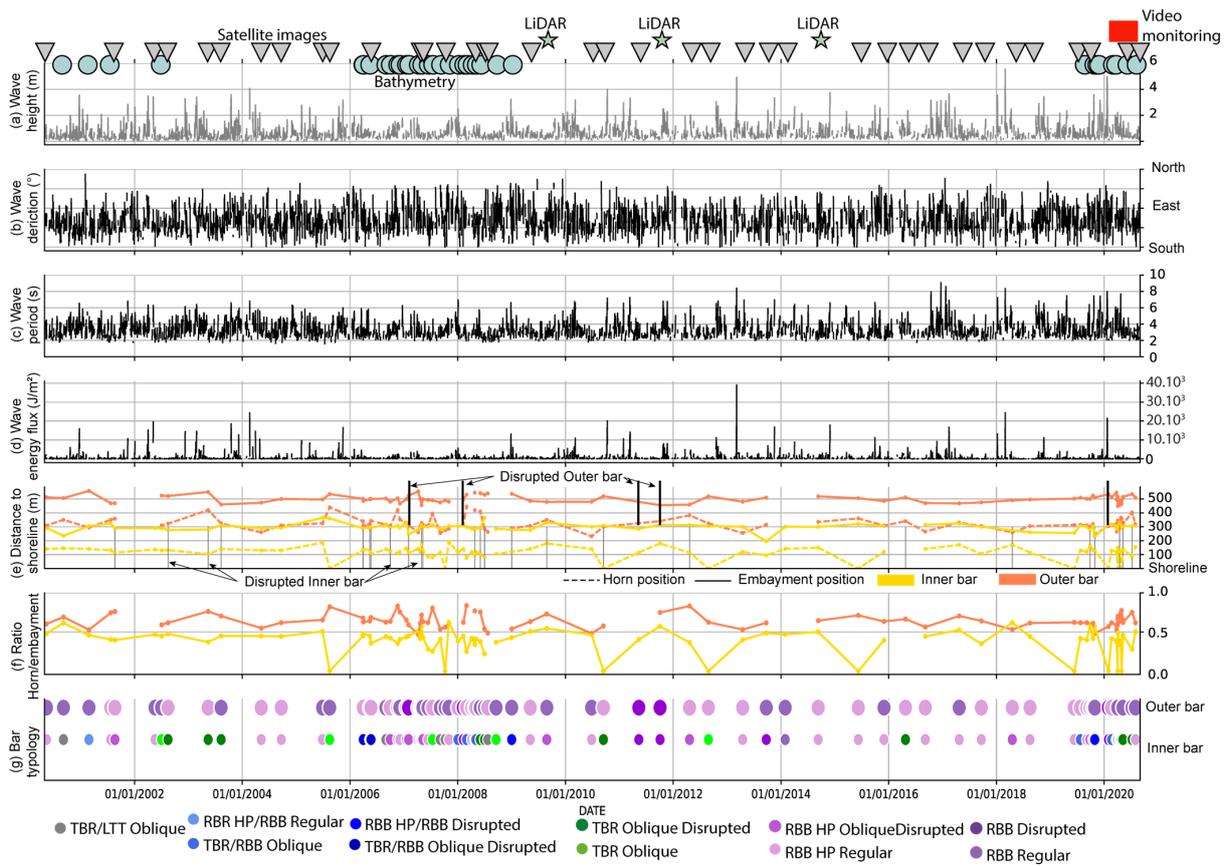
**Figure 6.** Time series of daily records of (**a**) wave height, periods and type of survey; round: bathymetry; triangle: satellite; star: LiDAR; red square: video monitoring period. (**b**) Wave direction given from shore normal. (**c**) Wave period. (**d**) Wave energy density. For reasons of clarity, periods during which waves are directed offshore are not shown. (**e**) Average distance between coastline and bar embayment (solid line) and between coastline and horn (dashed line) for inner (yellow) and outer (orange) bars. (**f**) Ratio of distance between coastline and horn to distance between coastline and embayment, with 1 representing less marked crescent shapes and 0 very marked. (**g**) Bar typology; outer bar on top and inner bar on bottom. In graphs (**e**,**f**,**g**), each point is an observation.
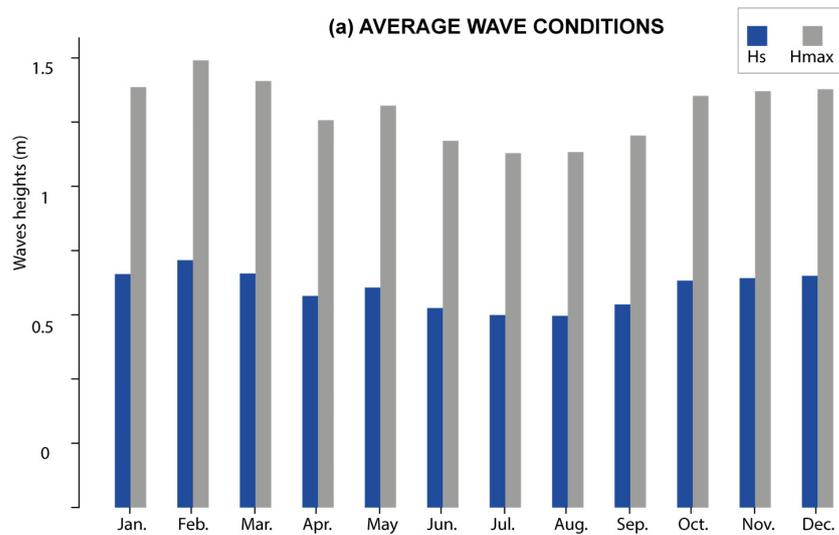


**Figure 7.** *Cont.*
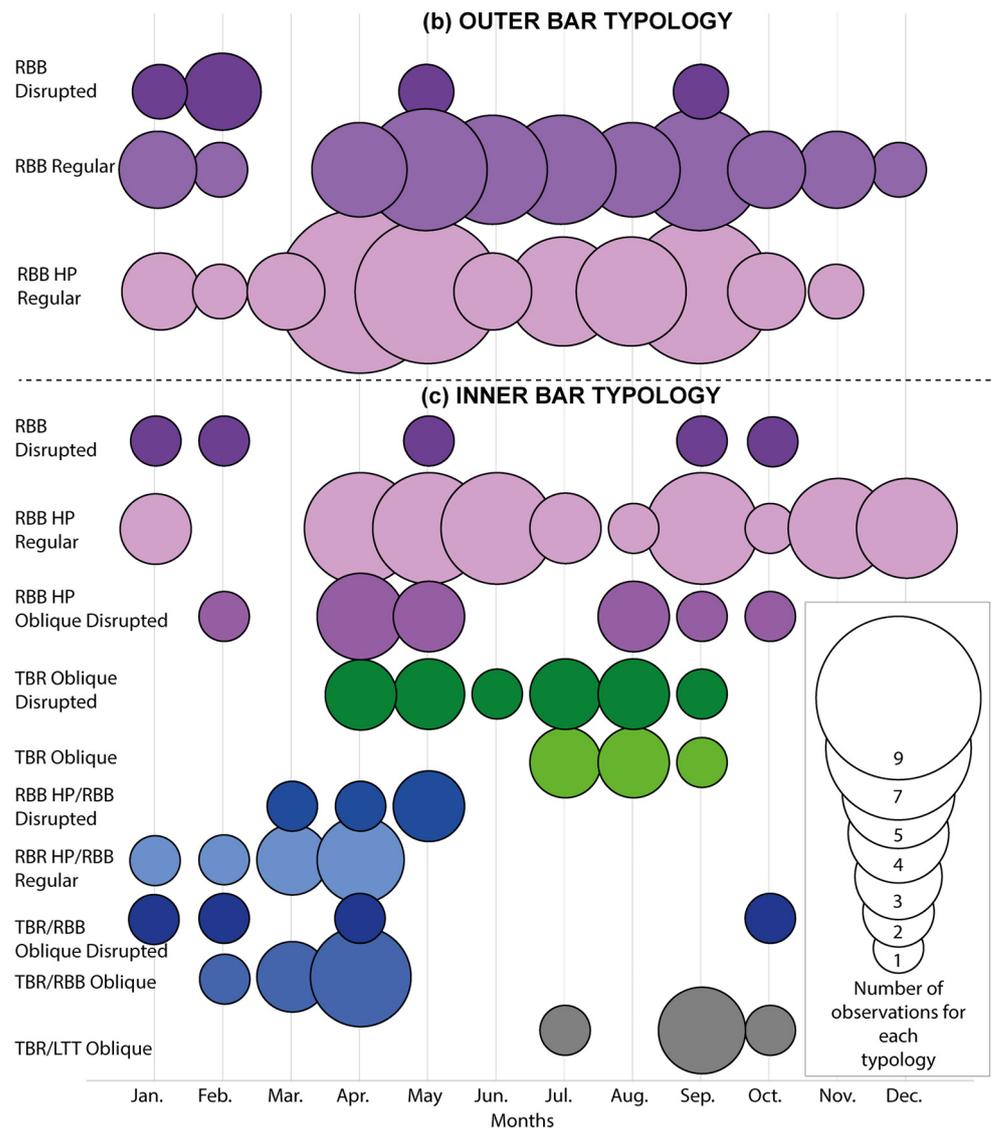
**Figure 7.** (**a**) Monthly averages of wave conditions over the study period. (**b**) Observations per month for the outer bar. (**c**) Observations per month for the inner bar. HP: high point.

### 4.3. Temporal Evolutions of Bar Typologies at the Event Scale

Table 1 shows the bar type at t + 1, thus highlighting the changes in bar type. Generally speaking, if we consider the evolution of the inner bar, most of the observed changes occur towards RBB types (RBB HP Regular, RBB HP Disrupted, RBB Disrupted; 43/79 observations), implying that the bar system is converging towards a dynamic equilibrium state. In detail, heterogeneous typologies remain primarily heterogeneous (stability) or may change towards RBB, i.e., towards the homogenization of the system in a RBB-type beach state. TBR types also change primarily to RBB or remain as TBR (indicating stability, despite applied forcing). RBB types show the greatest diversity of change, giving rise to all the other bar types. In the majority of cases, however, the typologies remain as RBB after a storm, illustrating once again the great resilience of these bars. To a secondary extent, these RBB types can change to TBR types or heterogeneous shapes. The graph (Figure 6g) shows, however, that if we wait long enough (several storm episodes), the inner bar always reverts to an RBB-type configuration.

**Table 1.** Changes in inner-bar typology during monitoring. On the left, the initial typology; on the top, the final typology. Cell coloring depends on the number of observations, darker for more observations.

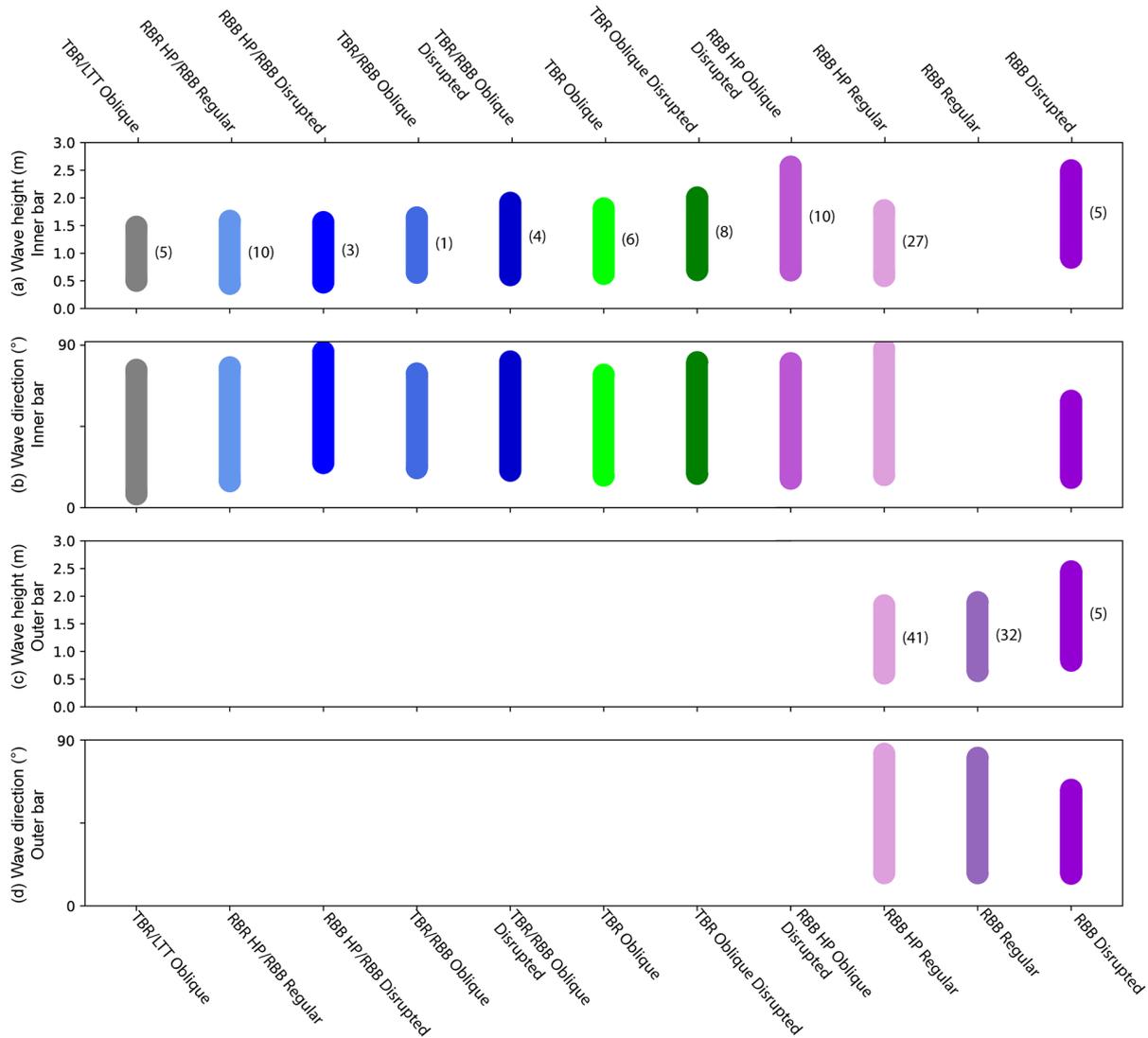| | | Final Typology | | | | | | | | | | |
| --- | --- | --- | --- | --- | --- | --- | --- | --- | --- | --- | --- | --- |
| | | TBR/LTT Oblique | TBR Oblique | TBR Oblique Disrupted | TBR/RBB Oblique | TBR/RBB Oblique Disrupted | RBB HP/RBB Regular | RBB HP/RBB Disrupted | RBB HP Regular | RBB HP Disrupted | RBB Disrupted | Total |
| Initial typology | TBR/LTT Oblique | 2 | 1 | | | | | | 2 | 1 | | 6 |
| | TBR Oilique | | | 1 | | 1 | 2 | | | 1 | | 5 |
| | TBR Oblique disrupted | 1 | | 4 | | | | | 3 | | 2 | 10 |
| | TBR/RBB Oblique | | | | 1 | 1 | 1 | | | | | 3 |
| | TBR/RBB Oblique disrupted | | | | | | 1 | | 1 | | | 2 |
| | RBB HP/RBB Regular | | | | | 1 | 2 | 1 | 3 | | | 7 |
| | RBB HP/RBB Disrupted | 1 | | | | | | 1 | | 2 | | 4 |
| | RBB HP Regular | 1 | 4 | 3 | | 1 | 1 | | 11 | 5 | 1 | 27 |
| | RBB HP Disrupted | | 1 | | | | 1 | 1 | 6 | | | 9 |
| | RBB Disrupted | | | | | | 2 | | 1 | 1 | 2 | 6 |
| | Total | 5 | 6 | 8 | 1 | 4 | 10 | 3 | 27 | 10 | 5 | 79 |

Here, a focus is brought to typology changes in relation to mean wave height and shore normal wave direction (Figure 8), highlighting the three most frequent final typologies (Table 1): RBB HP Regular (27/79 observations), RBB HP Oblique Disrupted (10/79 observations) and RBB HP/RBB Regular (10/79 observations).
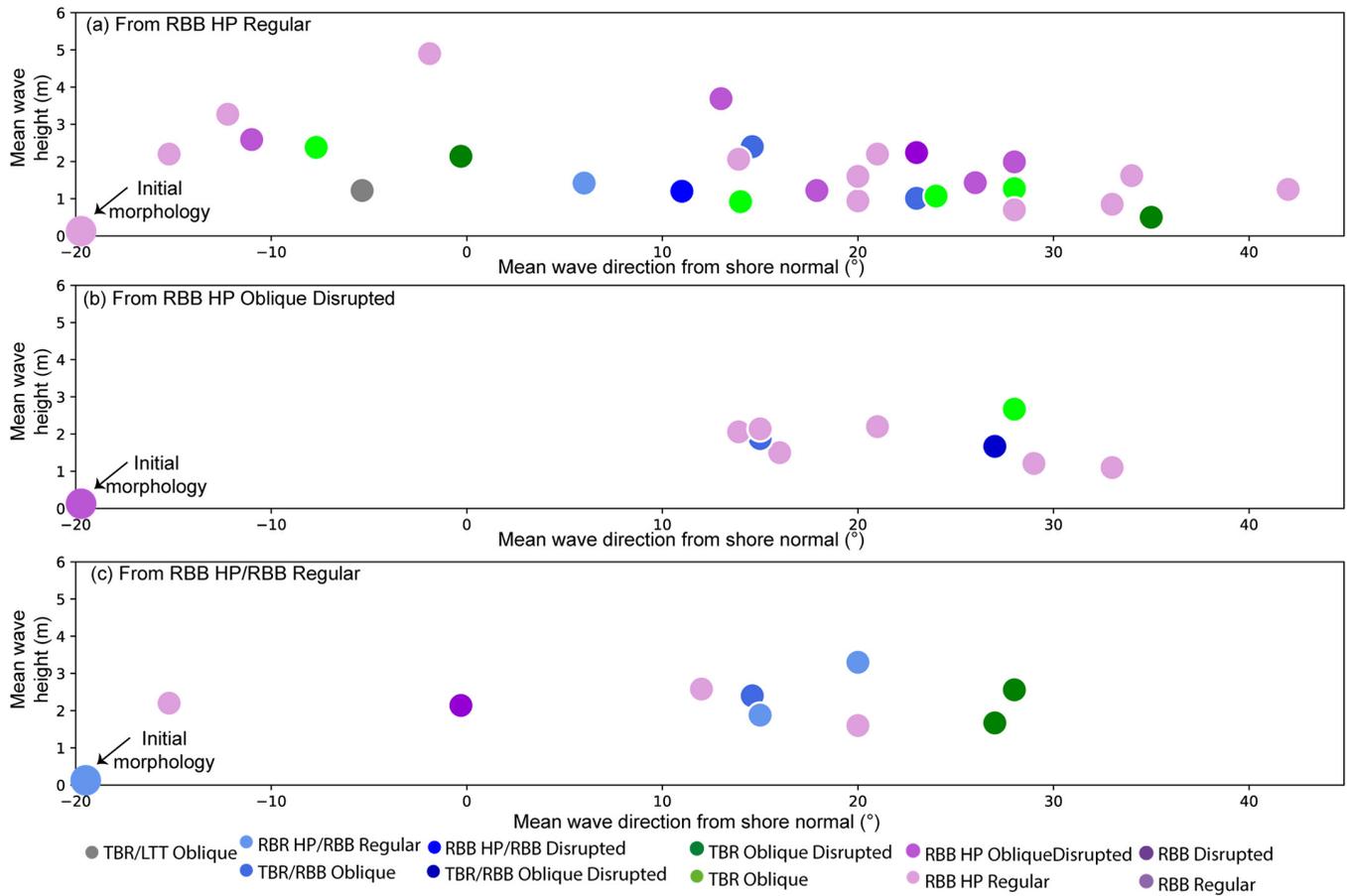


**Figure 8.** Possible changes in typology as a result of forcing conditions. The initial morphologies are (**a**) RBB HP; (**b**) RBB HP Oblique Disrupted; (**c**) Regular RBB HP/RBB Regular. Wave direction is given from shore normal; 0 indicates a direction perpendicular to the shoreline, and 90° is parallel (i.e., southerly).

(1) The RBB HP Regular typology is the one for which the most changes have been observed, accounting for almost 34% of the total (27/79 observations, Table 1). This is also the most common initial typology and the most stable: on 11 occasions during the monitoring period, this bar morphology withstood various forcing conditions without changing typology (Figure 8a). In the case where a change of typology is observed, seventeen of the twenty-seven cases are within the RBB category, while in seven of the twenty-seven cases, the change is to the TBR category (Table 1).

(2) Ten changes are observed towards the RBB HP Oblique Disrupted typology (nearly 13% of the total), which take place following energetic forcing conditions, with an average Hs between 1.5 and 3 m (Figure 8b). Once established, in six cases out of nine, these typologies will evolve towards a RBB HP regular typology (Table 1) by infilling of the rip channel.

(3) The heterogeneous typology RBB HP/RBB Regular (Table 1 and Figure 8c) remains either within the heterogeneous category (four/ten observations) or changes into RBB (four/ten observations) or TBR Oblique (two/ten observations), especially when the waves are very oblique to the shoreline (>20°, Figure 8c).

For the outer bar (Figure 9c,d), there appears to be an increase in energy between the RBB HP Regular, RBB Regular and RBB Disrupted typologies (Figure 9c), which occurs after periods of high-energy storms (Figure 6g). The wave direction shows little change between typologies but is concentrated around 30° with respect to perpendicular lines to the coast in the case of RBB Disrupted morphologies with waves coming from the southeast (Figure 9d). This sector is also where the most energetic storms are concentrated, which may explain the disrupted nature of the bars (Figure 1c).



**Figure 9.** Inner bar typologies according to (**a**) average wave height and (**b**) average wave direction. Outer bar typologies according to (**c**) average wave height and (**d**) average wave direction. In brackets, number of observations per typology. Wave direction is given by the shoreline normal.

For the inner bar (Figure 9a,b), the disrupted form shown by three typologies (TBR/RBB; TBR oblique and RBB) seems to be linked to slightly larger waves than for the uninterrupted form (Figures 9a and 10). Moreover, a wave direction > 20° seems to be linked to the emergence of inner bars showing 60% heterogeneous typologies (RBB HP/RBB Disrupted; TBR/RBB Oblique; TBR/RBB Oblique Disrupted) (Figures 9b and 10) associated with average wave heights of around 0.75 m.
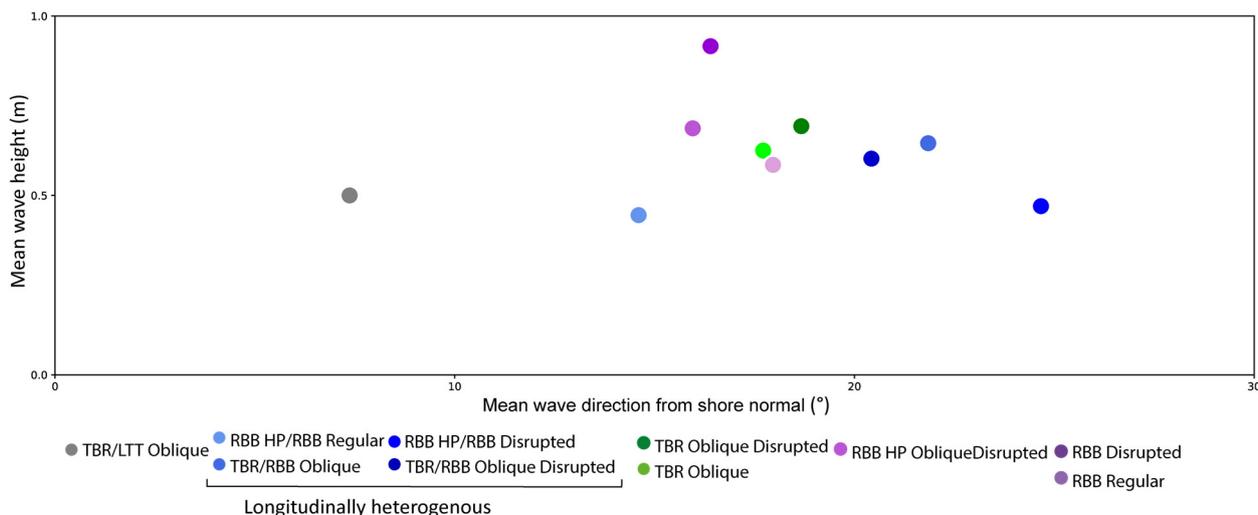
**Figure 10.** Typology of the inner bar according to average forcing conditions. Wave direction is given from shore normal.

### 4.4. Bar System Dynamics

4.4.1. Pattern Dynamics over 20 Years of Observation

For the outer bar, the cross-shore position of the embayment is relatively stable (Figure 6e), with only the horns fluctuating forward and backward within a mobility envelope of around 100 m (corresponding to 1/4 of the bar amplitude, Figure 6e). This bar corresponds to the same feature that has been mapped over the last 20 years and shows no seaward movement of the Net Offshore Migration type (Figure 11). The longshore position of the horns is contained within a mobility range of 150 m maximum (i.e., 1/4 of its mean wavelength) without any longshore migration of the entire system. In fact, the position of the outer bar in 2020 returned to the same position as recorded in 2000 (Figure 11). As observed with the cross-shore position, the longshore position of the horns oscillates around an equilibrium position. The crescentic pattern also remains constant over time and, therefore, shows no linearization (Figures 6f and 11). Bar breaches are rarely observed: five out of seventy-nine observations in 20 years (Figure 6e). However, it is important to note that since part of the monitoring is performed by visual photo interpretation of satellite images, the disrupted nature of the bar may be difficult to see.

On the other hand, the cross-shore position of the inner bar varies quite considerably, showing a noticeable mobility near the horns, which change their position within an envelope of 200 m (corresponding to 4/3 of the bar amplitude, Figure 6e) and can even come up against the coastline (Figure 6e). Although some movement is recorded, the bar never disappears by merging with the coastline or by seaward migration (Figure 6e), nor does it exhibit continuous longshore migration in the direction of longshore drift (to the north in the studied case; Figure 11), even under highly dynamic conditions. The inner bar merely oscillates around an equilibrium position over the 20 years of monitoring (Figure 6e). Bar breaches are quite common at the embayments (26 out of 79 observations in 20 years), particularly following winter storms (Figure 6e). Although the general pattern of the bars is always crescentic, strong variations in crescent amplitude are observed, although they never reach a linear state (Figure 6f). This pattern is most pronounced during periods when the horns are closest to the coastline (Figure 6e).
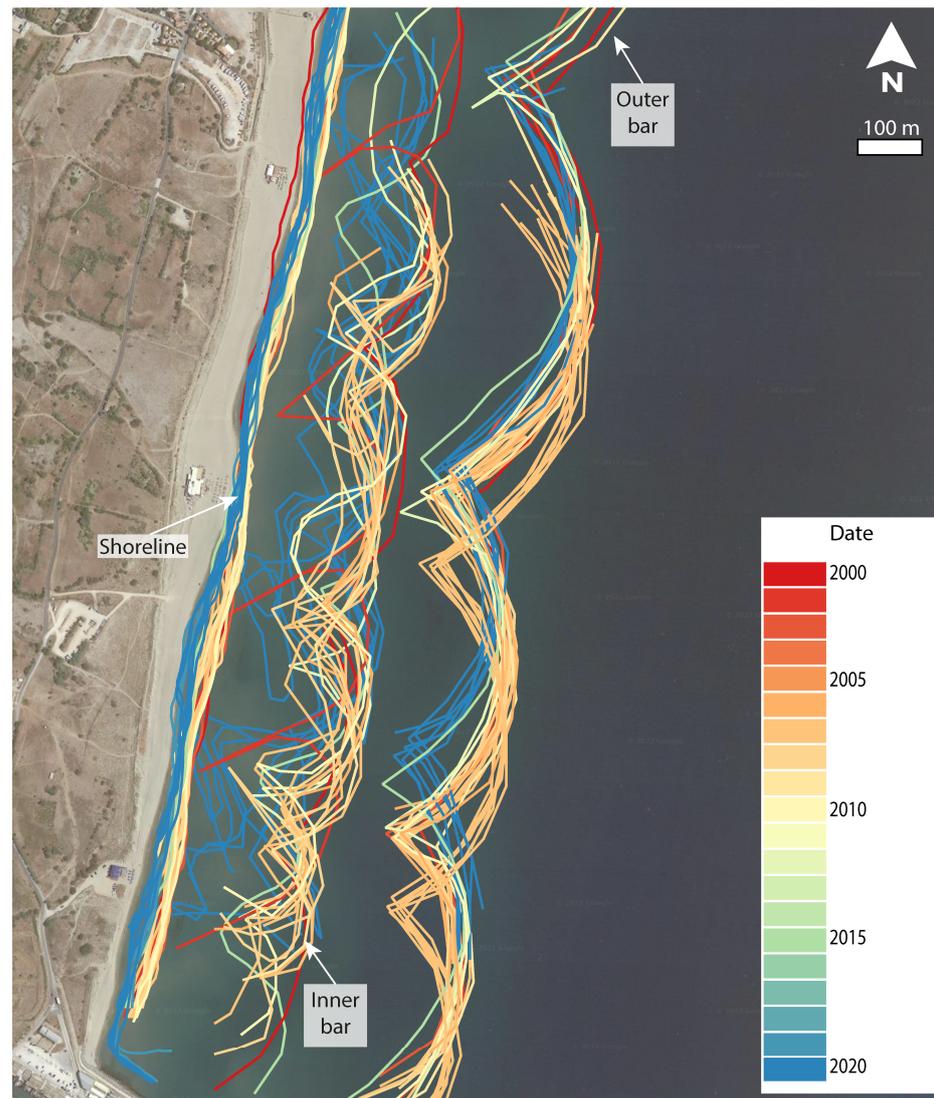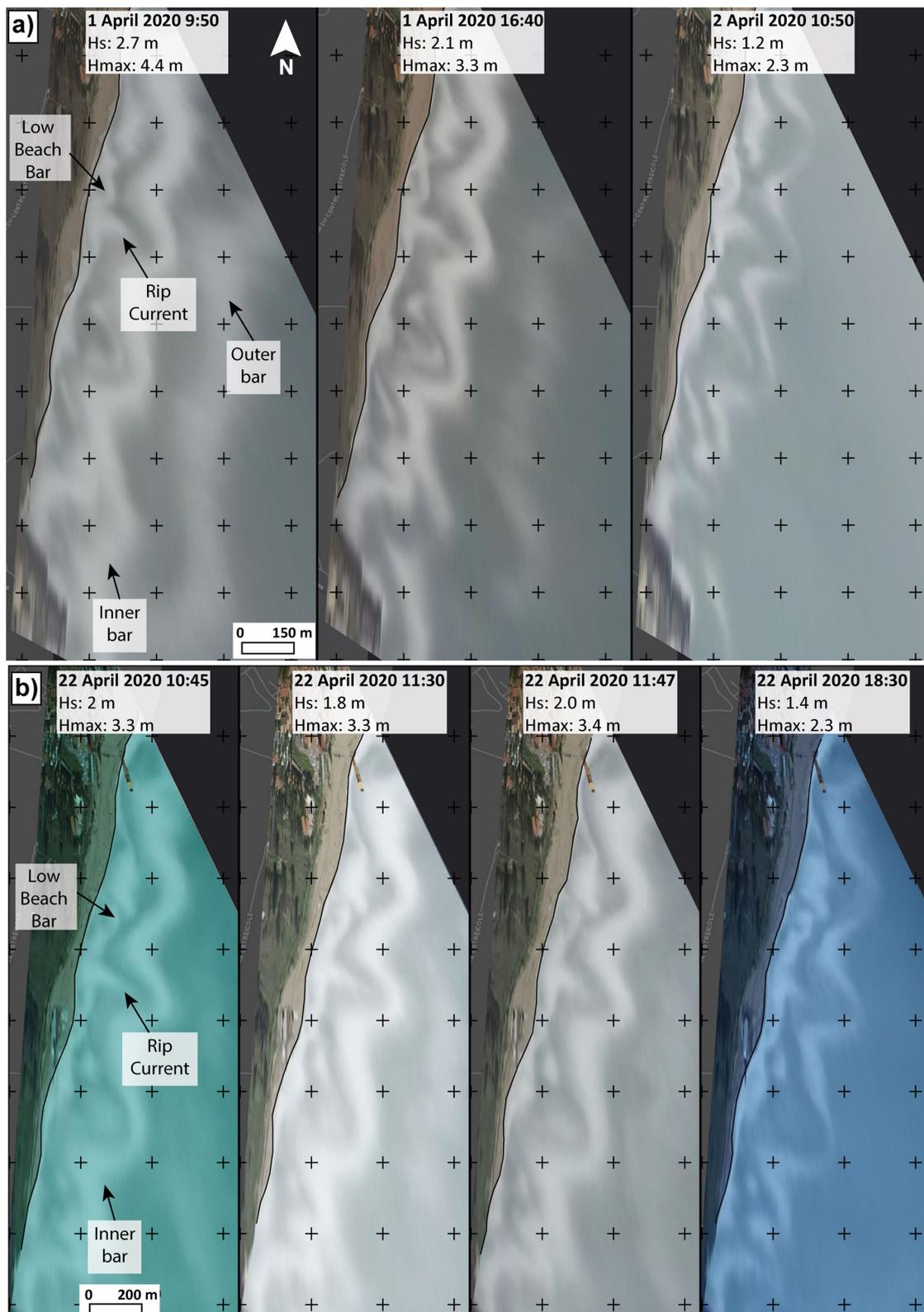
**Figure 11.** Position of inner and outer bars since 2000, color scale according to date.

4.4.2. Syn-Storm Evolution of Nearshore Bars

In the two series of averaged images presented here, each depicting a storm event (1 April 2020 and 22 April 2020) (Figure 12a,b), the inner bar typology remains homogeneous throughout the duration of each event, and the outer bar is only slightly impacted by the breakers (breaker marks are barely visible over the bar (Figure 12a), or not visible at all (Figure 12b)).

The multi-year monitoring shows that the inner bar is not linearized by either of these events, even with an Hmax greater than 3 m (Figure 6a). There appears to be very little syn-storm evolution of the inner bar since the RBB typology remains throughout the storm, in agreement with the observations shown in Figure 8. The crest of the inner bar remains at the same location on all images, indicating that no change of beach state occurred during these two storm events. The most notable morphological changes, however, appear to take place at the level of Low Beach Bars that were formed in very shallow waters connected with the shoreline and then disrupted during the second storm event (Figure 12b).

**Figure 12.** Leucate nearshore bars during two medium-intensity storms (**a**) 1 April 2024; (**b**) 22 April 2024. Black crosses are spaced 200 m apart.

*4.5. Coupling between Inner and Outer Bars*

Downwave coupling (when the two bars are in-phase opposition and slightly offset) was observed in 45% of cases; it is most prevalent for wave heights between 1 and 6 m,

with incoming wave directions between −20° (NE) and 30° (SE), and systematically when wave heights exceed 3 m, whatever the wave direction (Figure 13). For the remaining 55% of cases, for medium waves (between 0.5 and 2.5 m) with wave directions between 15° and 38°, the two bars are in-phase in 20% of observations. For waves of less than 2 m with a wave direction of 5° to 35°, the two bars are out-of-phase in 35% of observations.
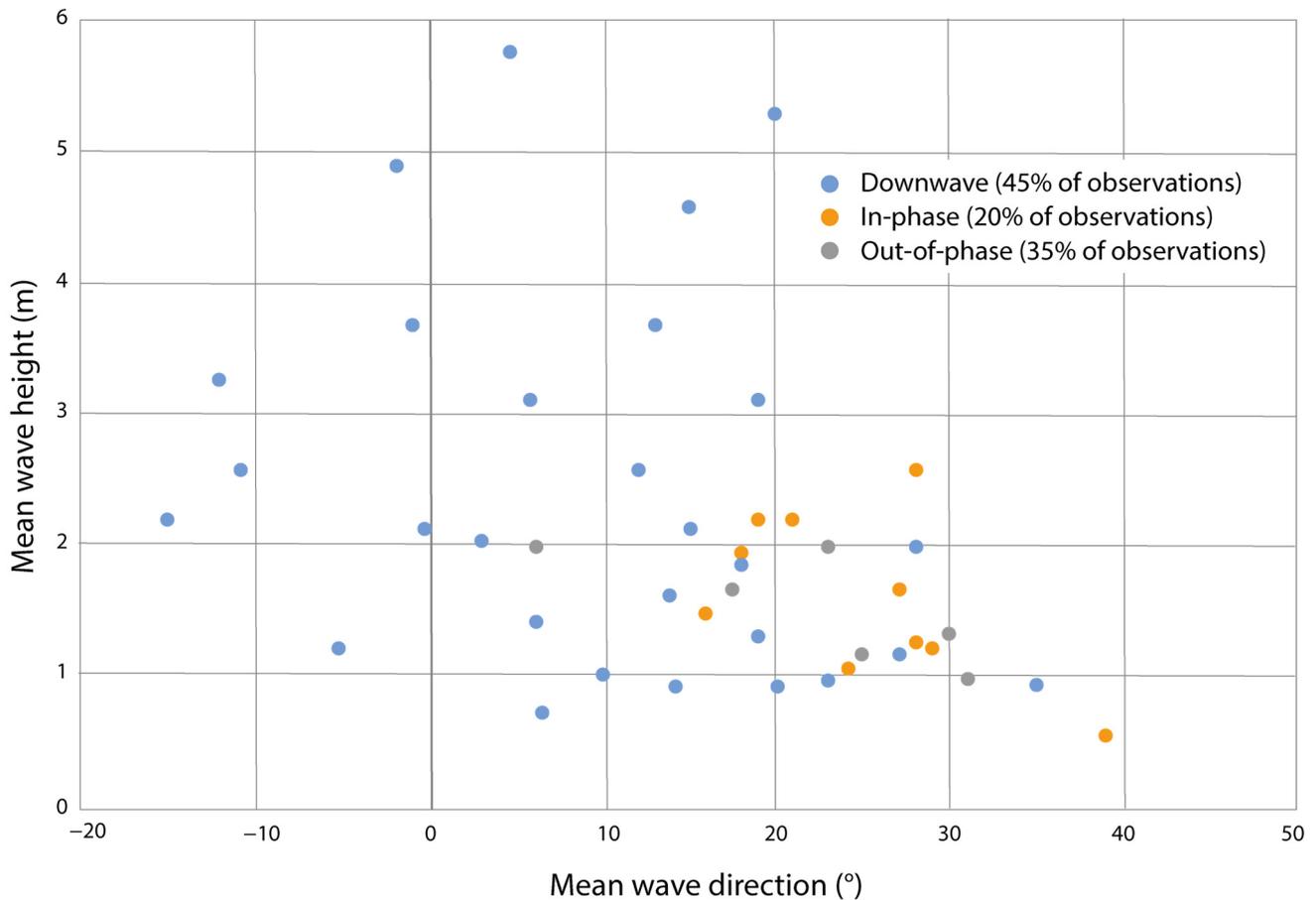


**Figure 13.** Type of coupling between outer and inner bars in relation to mean wave height and mean wave direction between two observations.

## 5. Discussion

### 5.1. Classification of Nearshore Bar Typology

The classification of bar typologies at the Leucate site is quite similar to what is already accepted in the literature [2,5,7,21,77]; however, there are some notable differences that will be discussed here. Low-energy waves (i.e., waves < 1 m) generate transverse bar typologies, while more energetic waves generate crescentic bars (Figure 14), revealing a seasonal signature. However, the slope, granulometry and energy characteristics of the Leucate site prevent the formation of linear bars, which represent the most energetic stage of the intermediate beach state [5,20,45,46,59,78]. The bars are thus always crescentic (Figure 14), unlike other more exposed Mediterranean sites outside the Gulf of Lions where the bars are only intermittently crescentic [51,79]. These typologies are grouped according to various sub-states based on already accepted classifications [13]: TBR/LTT, heterogeneous (RBB HP/RBB and TBR/RBB), TBR and RBB, showing either normal or oblique configurations, with uninterrupted or disrupted embayments (Figure 14). Heterogeneous typologies (RBB HP/RBB, TBR/RBB; Figure 5) are rarely described in the literature [13] but represent 25% of the inner bars observed here, which is in line with the results of previous studies (16.7%) in this part of the Gulf of Lions [13]. At Leucate, on the other hand, the outer bar never shows a heterogeneous configuration, whereas 34.9% of outer bars show this pattern over

the whole Gulf of Lions [13]. Locally, the larger space made available between the inner bar and the shoreline allows for the development of a proximal Low Beach Bar (LBB) system interspersed within the accommodation space (Figure 14), which is described in more detail in ref. [75].
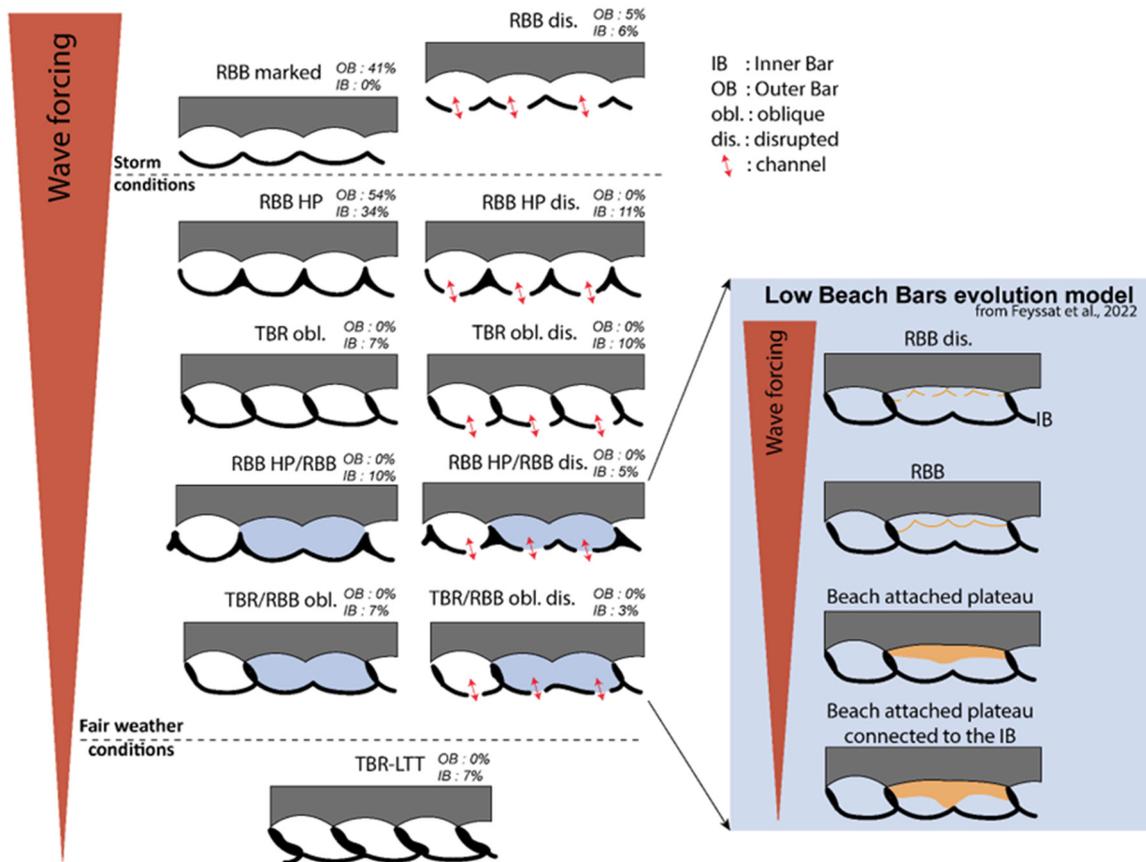


**Figure 14.** Typology of bars based on wave forcing intensity at the Leucate site; Feyssat et al., 2022 [75].

## 5.2. Nearshore Morphodynamics

Bar type combinations are more varied for the inner bar (ten typologies) than for the outer bar (three typologies).

Thus, the outer bar shows less typological variability (Figure 14); it is always of the RBB type, most often RBB HP Regular or RBB Regular. In the event of strong waves (Hs > 3 m), a breach may occur in the embayment (RBB Disrupted). The persistence of the RBB pattern is explained by the rarity of forcing conditions that can reach this bar (breaking waves: Hs > 4 m; [12]), which is quite commonly described at other sites [8,10,21,59]. Within the RBB typology, however, the bar shape can change if the storm episode is sufficiently energetic (change in horn shape and possible breaching). In contrast to single-bar sites, no linearization is observed during the most energetic episodes [20,46,59,78]. Furthermore, storm episodes at the Leucate site are not intense enough to reach a linearized beach state. At Leucate, Hm0 Q95% = 1.92 m compared to Hm0 Q95% = 4.08 m on the French Atlantic coast [80], where linearization episodes are observed on double-bar systems [11]. In the case of weaker forcing on the outer bar, the horns may migrate towards the coast [81,82] and connect to the underside of the inner bar embayments, resulting in a lower-energy form whose horn elongation is reminiscent of TBR substates [19,39,52,83].

The inner bar is more mobile, as is commonly accepted [8], and exhibits a wide variety of states. The TBR/LTT typology is a low-energy pattern (Figure 14), which is present in summer following long periods of fair weather. At the other end of the spectrum, the RBB Disrupted typology on the outer bar results from higher energy (Figure 14) conditions in

winter as well as following storms. In the case of storms of decadal recurrence (Waves > 6 m), the highly disrupted character of the inner bar system gives the impression that it has been reworked [84]. Between these two extremes, it is difficult to characterize the other bar typologies in terms of an energy scale, due to the transformation of the waves by refraction as it passes over the horns of the outer and inner bars [5,42,52,74]. On the other hand, according to accepted classifications [2,5,7], we can rank the typologies in order of increasing energy as follows: TBR/LTT, heterogeneous and oblique TBR (Figure 14), then RBB [52]. The presence of heterogeneous states implies that the entire bar pattern does not exhibit the same typology; a majority of the typologies (60%) appear to be created by medium-intensity wave conditions accompanied by rather high obliquity of wave incidence (>20°).

Attempts to associate one type of coupling between the bars with offshore forcing conditions are not conclusive at the event scale. However, the physical explanations for the different types of coupling (including the currents that generate them) appear to be in agreement with the results of previous studies carried out at the site [12,84,85]. The out-of-phase configuration develops during periods of low-intensity waves and becomes in-phase with more energetic waves, while downwave coupling (45% of observations) is associated with strongly oblique waves [23,39,54,62,63,65,66,86,87]. The dominance of this coupling configuration is explained here by the dominance of oblique mean forcing at the site (Figure 1d).

### 5.3. A Bar System Predominantly Characterized by RBB Typologies

One of the particularities of the study site is the high proportion of RBB types (100% outer bar; 51% inner bar; see Figure 14). In fact, even if the inner bar changes typology, it always tends to return to RBB types. The RBB-type outer bar imposes variable incident wave conditions along the coast that can control the longitudinal configuration of the inner bar [11,54,61,88,89]. Although changes are observed following intense forcing events at Leucate, several typologies are not smoothed out by a single event nor its decline, as observed at other sites [3]. The stability of the beach state and resilience of the RBB system at Leucate are unprecedented features—when compared with the literature—that reflect the unique character of this Mediterranean site.

One possible explanation for the prevalence of RBBs is that during low-intensity forcing conditions, which are the most common, the surf concentrates over the horns of the crescentic bars. This creates a return current opposing the bottom swell current directed towards the beach [30,84,85,90,91]. At Leucate, this mechanism may induce the growth of the horns and the establishment of the high points (Figure 14), thus concentrating a large proportion of the sediment and conferring great stability to these high points over time, similar to the mechanism behind the growth of transverse bars [74]. The onshore current created by wave asymmetry on these horns [92–94] can also explain their coastward migration, as observed in a downstate beach sequence [16,17,52,57,95,96]. However, Transverse Finger Bars connected to the coastline cannot be formed here as in other microtidal environments [74,97,98] due to the rather steep slope at Leucate (1° compared with the required threshold of <0.6°) and the coarser granulometry.

### 5.4. Low Mobility of the Bar System

Another special feature of the study site is the stability of the bars (both inner and outer), which show rather low-amplitude movements concentrated mainly at the crescent horns. These movements occur within a mobility envelope of around 150 m to 200 m longshore (corresponding to 1/2 of the wavelength of the inner bar in and 1/4 for the outer bar, Figure 11) and around 50 m to 150 m cross-shore (corresponding to 1/4 of the amplitude of the outer bar and 4/3 of that of the inner bar, Figure 11). In the case of Leucate, we can apply a model of cross-shore bar dynamics known as oscillation around a Point of Equilibrium (OPE), as already defined for linear bars in the northern part of the Gulf of Lions [37]. The OPE mechanism can also be evoked on another scale to describe

the longshore movements of the outer bar, which show a displacement of around 150 m to the north and then a return to the starting position within 20 years (Figure 11). This phenomenon is more difficult to observe on the inner bar, given the numerous changes in typology and horn location.

Despite the relatively low average forcing compared to the Atlantic Ocean, for example, bar wavelengths can reach significant dimensions here (L = 400 m for the inner bar and L = 600 m for the outer bar), similar to the systems in southwest France [8,99], which are located in a much more energetic environment (the Atlantic coast). The imposing size of these sedimentary bodies inevitably contributes to their inertia [100] and is also possibly controlled by the size of the outer bar, which is itself built up only during the strongest storms.

The slow evolution of the bars and the relatively minor syn-storm changes in morphology could also account for the absence of SPAWs (Shoreward Propagating Accretionary Waves; see ref. [9]) at the Leucate site, although such features can be observed at geographically close, albeit more energetic sites (Sète, 75 km farther north see [101]). These features usually emerge during rapid bifurcation of the bar horns (during a linearization episode, for example) and then migrate towards the coast [9,10,102]. The absence of linearization episodes may also explain the absence of SPAWs.

There are a few possible explanations for the relative stability of these systems. Firstly, the filtering effect of the outer bar on the incoming waves [5,42,52,74], thus limiting the energy transferred towards the shore. Secondly, although storms are potentially intense, they are short-lived (a few days, max.; see [73,103]) and are interspersed between long periods of calm, which also limits the amount of energy that can be transferred to the coast during these events. Due to the large size of the bars, it is possible that the storm duration is too short and the amount of energy delivered is insufficient to induce any rapid or major changes in beach morphology [104–106]. This hypothesis then raises the question of the initial formation of the bar system at the study site, one possibility being that it might have formed during extreme storm events, although this possibility cannot be validated or invalidated.

*5.5. Development and Evolution of Rip Channels*

During the most energetic events, it is possible to observe localized ruptures in the embayments of the inner and outer bars (Figure 14), creating channels that incise the crest of the bar and allowing for the expulsion of rip currents [95,107–109]. The latter is more frequent on the inner bar (35% of observations; Figure 14) than on the outer bar (5% of observations; Figure 14) and may give rise to asymmetrical inner bars, confirming that oblique waves are required for their formation [8,110,111].

Modeling studies on the crescentic bars of the Leucate sites [12,84] indicate the development of circulation cells on the inner bar with strong rip currents normal to the coast during storm events, causing the crest of the inner bar to break at its embayment. Wave heights above 4 m are required for these circulation cells to encompass the outer bar [12,84,85]. Once developed, these channels remain visible on bathymetric observations for long periods (up to several months for the outer bar; see ref. [13]) and can be subsequently reactivated. The persistence of the disrupted patterns can be explained by the morphological hysteresis in the evolution of the bars, which break up faster than they rebuild. This is because the accretionary mechanisms on these bars are lower-energy phenomena that take place over long periods of time. These bar ruptures subsequently resolve under the action of smaller waves without leading to the establishment of rip channels, leaving space available for the formation of TBR-type systems (TBR Oblique of the Aquitaine coast, known as Transverse Rip-Bars; see refs. [3,39,42,43,49,95,109,112,113]).

## 6. Conclusions

The morphodynamics of the Leucate double-crescent bar system have been studied over the last twenty years using bathymetric data supplemented by satellite and video

images. Due to the inertia of the system, we can determine the sequence of typologies and describe them in detail using bathymetry during periods of good weather between storm events.

During the monitoring period, 11 different bar typologies were identified, derived from those already described in the literature (LTT, TBR and RBB), with downwave coupling between bars in 45% of cases. The outer bar is always of the RBB type, most often RBB HP, and its position is relatively stable, although breaches can occur in the embayments. Movements of the outer bar horns are possible following particularly energetic episodes with cross-shore mobility of around 50 m. In addition, a northward to-and-fro movement of around 150 m (i.e., 1/4 of the wavelength) of the outer bar was visible over the 20 years of monitoring. On the other hand, the inner bar is more dynamic, exhibiting ten different typologies (categorized as TBR/LTT, heterogeneous, TBR and RBB), although, as with the outer bar, RBB substates are predominant. Breaching at the embayments is more common than on the outer bar, and the cross-shore movements of the horns, although similar in amplitude to those of the outer bar, represent a larger proportion relative to the size of the sedimentary body (i.e., 1/2 of the wavelength). Cross-shore movements of the inner bar are of the order of 200 m (for a bar amplitude of 150 m). While it is difficult to classify these bar typologies according to offshore wave forcing at the event scale, it appears more appropriate to do so at the seasonal scale. Low-energy summer waves are dominated by TBR/LTT and TBR, while RBB remains common throughout the year and becomes dominant in winter. The majority of disrupted bar configurations (inner and outer) are observed during this high-energy period. Due to the low recurrence of winter storms and long periods of fair weather, disrupted typologies can persist for several weeks to months. Eventually, however, the channels in the disrupted embayments are filled in. The return to less energetic periods at the end of winter is accompanied by the establishment of heterogeneous typologies (RBB HP/RBB, TBR/RBB), favorable to the development of a Low Beach Bar system intercalated between the inner bar and the shoreline at the level of the retreating horns. The seasonal nature of bar typologies does not lead to bar renewal through destruction/reconstruction. Morphological changes occur gradually on existing bars, with no new entities being created over the 20 years of monitoring. Over the multi-decade monitoring period, the inner/outer bar complex appears surprisingly stable.

Several areas of research could be explored to further develop the results of this work, in particular through modeling to gain a more detailed understanding of the establishment and behavior of heterogeneous states, and by extension the establishment of Low Beach Bars. This could also help to explore the development of the outer bar system, the dimensions of which are close to those observed in much more energetic environments (on the Atlantic coast). Lastly, as the coupling study was carried out on a relatively small stretch of beach compared with the size of the objects studied, it would be necessary to work on larger stretches of shoreline to reinforce the results obtained on bar couplings.

**Author Contributions:** Conceptualization, P.F., R.C. and N.R.; methodology, P.F., R.C., N.R., A.L., O.R. and B.H.; software, P.F.; investigation, P.F., R.C., N.R. and J.-P.B.; data curation, P.F.; writing—original draft preparation, P.F., R.C. and N.R.; writing—review and editing, P.F., R.C., N.R. and J.-P.B.; visualization, P.F.; supervision, R.C. and N.R.; funding acquisition, R.C. and N.R. All authors have read and agreed to the published version of the manuscript.

**Institutional Review Board Statement:** Not applicable.

**Informed Consent Statement:** Not applicable.

**Data Availability Statement:** The data that support the findings of this study are available from the corresponding author, upon reasonable request.

**Conflicts of Interest:** The authors declare no conflicts of interest.

## References

1. Wijnberg, K.M.; Kroon, A. Barred Beaches. *Geomorphology* **2002**, *48*, 103–120. [CrossRef]
2. Lippmann, T.C.; Holman, R.A. The Spatial and Temporal Variability of Sand Bar Morphology. *J. Geophys. Res.* **1990**, *95*, 11575. [CrossRef]
3. Phillips, M.S.; Harley, M.D.; Turner, I.L.; Splinter, K.D.; Cox, R.J. Shoreline Recovery on Wave-Dominated Sandy Coastlines: The Role of Sandbar Morphodynamics and Nearshore Wave Parameters. *Mar. Geol.* **2017**, *385*, 146–159. [CrossRef]
4. Angnuureng, D.B.; Almar, R.; Senechal, N.; Castelle, B.; Addo, K.A.; Marieu, V.; Ranasinghe, R. Shoreline Resilience to Individual Storms and Storm Clusters on a Meso-Macrotidal Barred Beach. *Geomorphology* **2017**, *290*, 265–276. [CrossRef]
5. Wright, L.D.; Short, A.D. Morphodynamic Variability of Surf Zones and Beaches: A Synthesis. *Mar. Geol.* **1984**, *56*, 93–118. [CrossRef]
6. Short, A.D.; Aagaard, T. Single and Multi-Bar Beach Change Models. *J. Coast. Res.* **1993**, 141–157.
7. Short, A.; Woodroffe, C. *The Coast of Australia*; Faculty of Science–Papers (Archive); Cambridge University Press: Cambridge, UK, 2009.
8. Castelle, B.; Bonneton, P.; Dupuis, H.; Sénéchal, N. Double Bar Beach Dynamics on the High-Energy Meso-Macrotidal French Aquitanian Coast: A Review. *Mar. Geol.* **2007**, *245*, 141–159. [CrossRef]
9. Wijnberg, K.; Holman, R. Video-Observation of Shoreward Propagating Accretionary Waves. In Proceedings of the RCEM 2007, Enschede, The Netherlands, 17–21 September 2007; Volume 2. [CrossRef]
10. Almar, R.; Castelle, B.; Ruessink, B.G.; Sénéchal, N.; Bonneton, P.; Marieu, V. Two- and Three-Dimensional Double-Sandbar System Behaviour under Intense Wave Forcing and a Meso–Macro Tidal Range. *Cont. Shelf Res.* **2010**, *30*, 781–792. [CrossRef]
11. Castelle, B.; Ruessink, B.G.; Bonneton, P.; Marieu, V.; Bruneau, N.; Price, T.D. Coupling Mechanisms in Double Sandbar Systems. Part 1: Patterns and Physical Explanation. *Earth Surf. Process. Landf.* **2010**, *35*, 476–486. [CrossRef]
12. Ferrer, P.; Certain, R.; Barusseau, J.P.; Gervais, M. Conceptual Modelling of a Double Crescentic Barred Coast (Leucate Beach, France). In Proceedings of the Coastal Dynamics 2009: Impacts of Human Activities on Dynamic Coastal Processes (with CD-ROM); World Scientific: Singapore, 2009; pp. 1–13.
13. Aleman, N.; Robin, N.; Certain, R.; Vanroye, C.; Barusseau, J.P.; Bouchette, F. Typology of Nearshore Bars in the Gulf of Lions (France) Using LIDAR Technology. *J. Coast. Res.* **2011**, *64*, 721–725.
14. Aleman, N.; Certain, R.; Robin, N.; Barusseau, J.-P. Morphodynamics of Slightly Oblique Nearshore Bars and Their Relationship with the Cycle of Net Offshore Migration. *Mar. Geol.* **2017**, *392*, 41–52. [CrossRef]
15. McCarroll, R.J.; Brander, R.W.; Turner, I.L.; Leeuwen, B.V. Shoreface Storm Morphodynamics and Mega-Rip Evolution at an Embayed Beach: Bondi Beach, NSW, Australia. *Cont. Shelf Res.* **2016**, *116*, 74–88. [CrossRef]
16. Komar, P.D. *Beach Processes and Sedimentation*; Prentice-Hall: Englewood Cliffs, NJ, USA, 1976; ISBN 978-0-13-072595-0.
17. Price, T.D.; Ruessink, B.G. State Dynamics of a Double Sandbar System. *Cont. Shelf Res.* **2011**, *31*, 659–674. [CrossRef]
18. Nnafie, A.; van Andel, N.; de Swart, H. Modelling the Impact of a Time-Varying Wave Angle on the Nonlinear Evolution of Sand Bars in the Surf Zone. *Earth Surf. Process. Landf.* **2020**, *45*, 2603–2612. [CrossRef]
19. Castelle, B.; Masselink, G. Morphodynamics of Wave-Dominated Beaches. *Camb. Prism. Coast. Futures* **2022**, *1*, e1. [CrossRef]
20. Holman, R.; Symonds, G.; Thornton, E.; Ranasinghe, R. Rip Spacing and Persistence on an Embayed Beach. *J. Geophys. Res.* **2006**, *111*. [CrossRef]
21. van Enckevort, I.M.J. Observations of Nearshore Crescentic Sandbars. *J. Geophys. Res.* **2004**, *109*, C06028. [CrossRef]
22. Ojeda, E.; Guillén, J.; Ribas, F. Dynamics of Single-Barred Embayed Beaches. *Mar. Geol.* **2011**, *280*, 76–90. [CrossRef]
23. de Swart, R.; Ribas, F.; Calvete, D.; Simarro, G.; Guillen, J. Observations of Megacusp Dynamics and Their Coupling with Crescentic Bars at an Open, Fetch-limited Beach. *Earth Surf. Process. Landf.* **2022**, *47*, 3180–3198. [CrossRef]
24. Goldsmith, V.; Bowman, D.; Kiley, K. Sequential Stage Development of Crescentic Bars: Hahoterim Beach, Southeastern Mediterranean. *J. Sediment. Res.* **1982**, *52*, 233–249. [CrossRef]
25. Armaroli, C.; Ciavola, P. Dynamics of a Nearshore Bar System in the Northern Adriatic: A Video-Based Morphological Classification. *Geomorphology* **2011**, *126*, 201–216. [CrossRef]
26. Parlagreco, L.; Melito, L.; Devoti, S.; Perugini, E.; Zitti, G.; Brocchini, M. Monitoring for Coastal Resilience: Preliminary Data from Five Italian Sandy Beaches. *Sensors* **2019**, *19*, 1854. [CrossRef]
27. Melito, L.; Parlagreco, L.; Perugini, E.; Postacchini, M.; Devoti, S.; Soldini, L.; Zitti, G.; Liberti, L.; Brocchini, M. Sandbar Dynamics in Microtidal Environments: Migration Patterns in Unprotected and Bounded Beaches. *Coast. Eng.* **2020**, *161*, 103768. [CrossRef]
28. Fanini, L.; Defeo, O.; Elliott, M. Advances in Sandy Beach Research—Local and Global Perspectives. *Estuar. Coast. Shelf Sci.* **2020**, *234*, 106646. [CrossRef]

29.   Power, H.E.; Pomeroy, A.W.M.; Kinsela, M.A.; Murray, T.P. Research Priorities for Coastal Geoscience and Engineering: A Collaborative Exercise in Priority Setting From Australia. *Front. Mar. Sci.* **2021**, *8*, 252. [CrossRef]

30.   Brocchini, M. Wave-forced Dynamics in the Nearshore River Mouths, and Swash Zones. *Earth Surf. Process. Landf.* **2020**, *45*, 75–95. [CrossRef]

31.   Roelvink, J.A.; Stive, M.J.F. Bar-Generating Cross-Shore Flow Mechanisms on a Beach. *J. Geophys. Res. Ocean.* **1989**, *94*, 4785–4800. [CrossRef]

32.   Gallagher, E.L.; Elgar, S.; Guza, R.T. Observations of Sand Bar Evolution on a Natural Beach. *J. Geophys. Res.* **1998**, *103*, 3203–3215. [CrossRef]

33.   Ruessink, B.G.; Kroon, A. The Behaviour of a Multiple Bar System in the Nearshore Zone of Terschelling, The Netherlands: 1965–1993. *Mar. Geol.* **1994**, *121*, 187–197. [CrossRef]

34.   Aleman, N.; Robin, N.; Certain, R.; Barusseau, J.-P.; Gervais, M. Net Offshore Bar Migration Variability at a Regional Scale: Inter-Site Comparison (Languedoc-Roussillon, France). *J. Coast. Res.* **2013**, *165*, 1715–1720. [CrossRef]

35.   Shand, R.D.; Bailey, D.G. A Review of Net Offshore Migration with Photographic Illustrations from Wanganui. *J. Coast. Res.* **1999**, *15*, 365–378.

36.   Ruessink, B.G.; Pape, L.; Turner, I.L. Daily to Interannual Cross-Shore Sandbar Migration: Observations from a Multiple Sandbar System. *Cont. Shelf Res.* **2009**, *29*, 1663–1677. [CrossRef]

37.   Certain, R.; Barusseau, J.-P. Conceptual Modelling of Sand Bars Morphodynamics for a Microtidal Beach (Sète, France). *Bull. Société Géologique Fr.* **2005**, *176*, 343–354. [CrossRef]

38.   Coco, G.; Murray, B.; Ashton, A.D. Chapter 13—Rhythmic Patterns in the Surfzone. In *Sandy Beach Morphodynamics*; Elsevier: Amsterdam, The Netherlands, 2020; pp. 297–312.

39.   Calvete, D.; Dodd, N.; Falqués, A.; van Leeuwen, S. Morphological Development of Rip Channel Systems: Normal and near-Normal Wave Incidence. *J. Geophys. Res* **2005**, *110*. [CrossRef]

40.   Castelle, B.; Ruessink, B.G. Modeling Formation and Subsequent Nonlinear Evolution of Rip Channels: Time-Varying versus Time-Invariant Wave Forcing. *J. Geophys. Res. Earth Surf.* **2011**, *116*. [CrossRef]

41.   Deigaard, R.; Drønen, N.K.; Fredsøe, J.; Hjelmager Jensen, J.; Jørgensen, M.P. A Morphological Stability Analysis for a Long Straight Barred Coast. *Coast. Eng.* **1999**, *36*, 171–195. [CrossRef]

42.   Garnier, R.; Calvete, D.; Falqués, A.; Dodd, N. Modelling the Formation and the Long-Term Behavior of Rip Channel Systems from the Deformation of a Longshore Bar. *J. Geophys. Res. Ocean.* **2008**, *113*. [CrossRef]

43.   Reniers, A.J.H.M.; Roelvink, J.A.; Thornton, E.B. Morphodynamic Modeling of an Embayed Beach under Wave Group Forcing. *J. Geophys. Res. Ocean.* **2004**, *109*. [CrossRef]

44.   Smit, M.W.J.; Reniers, A.; Ruessink, G.; Roelvink, D.J.A. The Morphological Response of a Nearshore Double Sandbar System to Constant Wave Forcing. *Coast. Eng.* **2008**, *55*, 761–770. [CrossRef]

45.   Contardo, S.; Symonds, G. Sandbar Straightening under Wind-Sea and Swell Forcing. *Mar. Geol.* **2015**, *368*, 25–41. [CrossRef]

46.   Garnier, R.; Falqués, A.; Calvete, D.; Thiébot, J.; Ribas, F. A Mechanism for Sandbar Straightening by Oblique Wave Incidence. *Geophys. Res. Lett.* **2013**, *40*, 2726–2730. [CrossRef]

47.   Calvete, D.; Coco, G.; Falqués, A.; Dodd, N. (Un)Predictability in Rip Channel Systems. *Geophys. Res. Lett.* **2007**, *34*. [CrossRef]

48.   Smit, M.W.J.; Reniers, A.J.H.M.; Stive, M.J.F. Role of Morphological Variability in the Evolution of Nearshore Sandbars. *Coast. Eng.* **2012**, *69*, 19–28. [CrossRef]

49.   Tiessen, M.; Dodd, N.; Garnier, R. Development of Crescentic Bars for a Periodically Perturbed Initial Bathymetry. *J. Geophys. Res.* **2011**, *116*, 4016. [CrossRef]

50.   Castelle, B.; Bonneton, P.; Butel, R. Modélisation du festonnage des barres sableuses d'avant-côte: Application à la côte aquitaine, France. *Comptes Rendus Geosci.* **2006**, *338*, 795–801. [CrossRef]

51.   de Swart, R.L.; Ribas, F.; Simarro, G.; Guillén, J.; Calvete, D. The Role of Bathymetry and Directional Wave Conditions on Observed Crescentic Bar Dynamics. *Earth Surf. Process. Landf.* **2021**, *46*, 3252–3270. [CrossRef]

52.   Dubarbier, B.; Castelle, B.; Ruessink, G.; Marieu, V. Mechanisms Controlling the Complete Accretionary Beach State Sequence. *Geophys. Res. Lett.* **2017**, *44*, 5645–5654. [CrossRef]

53.   Marchesiello, P.; Chauchat, J.; Shafiei, H.; Almar, R.; Benshila, R.; Dumas, F.; Debreu, L. 3D Wave-Resolving Simulation of Sandbar Migration. *Ocean Model.* **2022**, *180*, 102127. [CrossRef]

54.   Coco, G.; Calvete, D.; Ribas, F.; de Swart, H.E.; Falqués, A. Emerging Crescentic Patterns in Modelled Double Sandbar Systems under Normally Incident Waves. *Earth Surf. Dyn.* **2020**, *8*, 323–334. [CrossRef]

55.   Castelle, B.; Bonneton, P.; Butel, R. Modélisation de La Morphodynamique Des Barres En Croissant de La Côte Aquitaine. In Proceedings of the VIIIèmes Journées Nationales Génie Civil–Génie Côtier, Compiègne, France, 7–9 September 2004; p. 174, ISBN 978-2-9505787-7-8.

56.   D'Alessandro, F.; Tomasicchio, G.R. Wave–Dune Interaction and Beach Resilience in Large-Scale Physical Model Tests. *Coast. Eng.* **2016**, *116*, 15–25. [CrossRef]

57.   Ranasinghe, R.; Symonds, G.; Black, K.; Holman, R. Morphodynamics of Intermediate Beaches: A Video Imaging and Numerical Modelling Study. *Coast. Eng.* **2004**, *51*, 629–655. [CrossRef]

58.   Hom-ma, M.; Sonu, C. Rhythmic Pattern of Longshore Bars Related to Sediment Characteristics. *Coast. Eng. Proc.* **1962**, *1*, 16. [CrossRef]

59. Short, A.D. *Handbook of Beach and Shoreface Morphodynamics*; John Wiley: Oxford, UK, 1999; ISBN 0-471-96570-7.

60. Ruessink, B.G.; Coco, G.; Ranasinghe, R.; Turner, I.L. Coupled and Noncoupled Behavior of Three-Dimensional Morphological Patterns in a Double Sandbar System. *J. Geophys. Res. Ocean.* **2007**, *112*. [CrossRef]

61. Price, T.D.; Ruessink, B.G.; Castelle, B. Morphological Coupling in Multiple Sandbar Systems—A Review. *Earth Surf. Dynam.* **2014**, *2*, 309–321. [CrossRef]

62. Sonu, C. Field Observation of Nearshore Circulation and Meandering Currents. *J. Geophys. Res. (1896–1977)* **1972**, *77*, 3232–3247. [CrossRef]

63. Price, T.; Rutten, J.; Ruessink, G. Coupled Behaviour within a Double Sandbar System. *J. Coast. Res.* **2011**, *SI64*, 125–129.

64. Thiébot, J.; Idier, D.; Garnier, R.; Falqués, A.; Ruessink, B.G. The Influence of Wave Direction on the Morphological Response of a Double Sandbar System. *Cont. Shelf Res.* **2012**, *32*, 71–85. [CrossRef]

65. Balouin, Y.; Tesson, J.; Gervais, M. Cuspate Shoreline Relationship with Nearshore Bar Dynamics during Storm Events—Field Observations at Sete Beach, France. *J. Coast. Res.* **2013**, *65*, 440–445. [CrossRef]

66. van de Lageweg, W.I.; Bryan, K.R.; Coco, G.; Ruessink, B.G. Observations of Shoreline–Sandbar Coupling on an Embayed Beach. *Mar. Geol.* **2013**, *344*, 101–114. [CrossRef]

67. Lamy, A.; Robin, N.; Smyth, T.; Hesp, P.; René, C.; Pierre, F.; Raynal, O.; Hebert, B. Impact of Temporal Beach Grain Size Variability on Aeolian Sediment Transport and Topographic Evolution in a Microtidal Environment. *Geomorphology* **2024**, *453*, 109126. [CrossRef]

68. Lamy, A.; Smyth, T.; Robin, N.; Hesp, P. Using Computational Fluid Dynamics (CFD) to Investigate Airflow and Sand Transport on a Human-Made Coastal Foredune Dominated by Offshore Wind: Impact of the Shape Variability. *Coast. Eng.* **2024**, *191*, 104534. [CrossRef]

69. Aleman, N.; Robin, N.; Certain, R.; Anthony, E.J.; Barusseau, J.P. Longshore Variability of Beach States and Bar Types in a Microtidal, Storm-Influenced, Low-Energy Environment. *Geomorphology* **2015**, *241*, 175–191. [CrossRef]

70. Certain, R. Morphodynamique D'une Côte Sableuse Microtidale à Barres: Le Golfe du Lion (Languedoc-Roussillon). Ph.D. Thesis, Université de Perpignan, Perpignan, France, 2002.

71. Mendoza, E.; Jiménez, J. Storm-Induced Beach Erosion Potential on the Catalonian Coast. *J. Coast. Res. SI* **2006**, *48*, 81–88.

72. Cerema Centre D'Étude et D'Expertise Sur Les Risques, L'Environnement, la Mobilité et L'Aménagement; Dreal Languedoc-Roussillon. Observatoire Océanologique de Banyuls CANDHIS—Détail de La Campagne 01101—Leucate. Available online: https://candhis.cerema.fr/_public_/campagne.php?Y2FtcD0wMTEwMQ== (accessed on 1 April 2019).

73. Guizien, K. Spatial Variability of Wave Conditions in the Gulf of Lions (NW-Mediterranean Sea). *Life Environ.* **2009**, *59*, 261–270.

74. Falqués, A.; Ribas, F.; Mujal-Colilles, A.; Puig-Polo, C. A New Morphodynamic Instability Associated with Cross-Shore Transport in the Nearshore. *Geophys. Res. Lett.* **2021**, *48*, e2020GL091722. [CrossRef]

75. Feyssat, P.; Certain, R.; Robin, N.; Raynal, O.; Lamy, A.; Hebert, B. Low Beach Bars: A Discontinuous Subtidal System of Proximal Bars within Mediterranean Low Microtidal Crescentics Systems. In Proceedings of the XVIIèmes Journées Nationales Génie Côtier—Génie Civil, Chatou, France, 11–13 October 2022; p. 10.

76. Vos, K.; Splinter, K.; Harley, M.; Simmons, J.; Turner, I. CoastSat: A Google Earth Engine-Enabled Python Toolkit to Extract Shorelines from Publicly Available Satellite Imagery. *Environ. Model. Softw.* **2019**, *122*, 104528. [CrossRef]

77. Caballeria, M.; Coco, G.; Falqués, A.; Huntley, D.A. Self-Organization Mechanisms for the Formation of Nearshore Crescentic and Transverse Sand Bars. *J. Fluid Mech.* **2002**, *465*, 379–410. [CrossRef]

78. Splinter, K.; Holman, R.; Plant, N. A Behavior-Oriented Dynamic Model for Sandbar Migration and 2DH Evolution. *J. Geophys. Res.* **2011**, *116*, C01020. [CrossRef]

79. de Swart, R.; Ribas, F.; Calvete, D.; Simarro, G.; Guillén, J. Characteristics and Dynamics of Crescentic Bar Events at an Open, Mediterranean Beach. In Proceedings of the EGU2020: Sharing Geoscience, Online, 8 May 2020.

80. Kergadallan, X. *Candhis: Analyses 2022 Des États de Mer Tome 1—Mer Du Nord, Manche et Atlantique*; Cerema: Bron, France, 2022.

81. van Enckevort, I.M.J.; Ruessink, B.G. Video Observations of Nearshore Bar Behaviour. Part 2: Alongshore Non-Uniform Variability. *Cont. Shelf Res.* **2003**, *23*, 513–532. [CrossRef]

82. Vidal, J.; Ruiz de Alegria-Arzaburu, A. Variability of Sandbar Morphometrics over Three Seasonal Cycles on a Single-Barred Beach. *Geomorphology* **2019**, *333*, 61–72. [CrossRef]

83. Garnier, R.; Dodd, N.; Falqués, A.; Calvete, D. Mechanisms Controlling Crescentic Bar Amplitude. *J. Geophys. Res. Earth Surf.* **2010**, *115*. [CrossRef]

84. Ferrer, P.; Certain, R.; Adloff, F.; Bouchette, F.; Meulé, S.; Robin, N. Hydrodynamics over a Microtidal Double Crescentic Barred Beach in Low Energetic Conditions (Leucate Beach, France). *J. Coast. Res.* **2011**, *5*, 2032–2036.

85. Bujan, N. Application d'un Modèle de Circulation Quasi-Tridimensionnel Littoral à la Dynamique des Plages du Languedoc-Roussillon. Ph.D. Thesis, Université Montpellier II-Sciences et Techniques du Languedoc, Montpellier, France, 2009.

86. Orzech, M.D.; Reniers, A.J.H.M.; Thornton, E.B.; MacMahan, J.H. Megacusps on Rip Channel Bathymetry: Observations and Modeling. *Coast. Eng.* **2011**, *58*, 890–907. [CrossRef]

87. Macmahan, J.; Brown, J.; Brown, J.; Thornton, E.; Reniers, A.; Stanton, T.; Henriquez, M.; Gallagher, E.; Morrison, J.; Austin, M.; et al. Mean Lagrangian Flow Behavior on an Open Coast Rip-Channeled Beach: A New Perspective. *Mar. Geol.* **2010**, *268*, 1–15. [CrossRef]

88. Coco, G.; Murray, A.B. Patterns in the Sand: From Forcing Templates to Self-Organization. *Geomorphology* **2007**, *91*, 271–290. [CrossRef]
89. Nnafie, A.; de Swart, H.E.; Falqués, A.; Calvete, D. Long-Term Morphodynamics of a Coupled Shelf-Shoreline System Forced by Waves and Tides, a Model Approach. *J. Geophys. Res. Earth Surf.* **2021**, *126*, e2021JF006315. [CrossRef]
90. Aagaard, T.; Masselink, G. The Surf Zone. In *Handbook of Beach and Shoreface Morphodynamics*; Wiley: Chichester, UK, 1999; ISBN 978-0-471-96570-1.
91. Masselink, G.; Scott, T.; Austin, M.; Russell, P. Experience the Power of Rip Currents. Bang Goes The Theory, Episode 2. 2011. Available online: https://www.researchgate.net/publication/235651705_Experience_the_power_of_rip_currents_Bang_Goes_The_Theory_Episode_2 (accessed on 2 May 2024).
92. Hoefel, F.; Elgar, S. Wave-Induced Sediment Transport and Sandbar Migration. *Science* **2003**, *299*, 1885–1887. [CrossRef]
93. Berni, C.; Barthélemy, E.; Michallet, H. Surf Zone Cross-Shore Boundary Layer Velocity Asymmetry and Skewness: An Experimental Study on a Mobile Bed. *J. Geophys. Res. Ocean.* **2013**, *118*, 2188–2200. [CrossRef]
94. Fernández-Mora, A.; Calvete, D.; Falqués, A.; de Swart, H.E. Onshore Sandbar Migration in the Surf Zone: New Insights into the Wave-Induced Sediment Transport Mechanisms. *Geophys. Res. Lett.* **2015**, *42*, 2869–2877. [CrossRef]
95. Brander, R.W. Field Observations on the Morphodynamic Evolution of a Low-Energy Rip Current System. *Mar. Geol.* **1999**, *157*, 199–217. [CrossRef]
96. Shepard, F.P.; Inman, D.L. *Nearshore Circulation*; Coastal Engineering Proceedings; Scripps Institution of Oceanography: La Jolla, CA, USA, 1950; pp. 50–59. [CrossRef]
97. Ribas, F.; Kroon, A. Characteristics and Dynamics of Surfzone Transverse Finger Bars. *J. Geophys. Res. Earth Surf.* **2007**, *112*. [CrossRef]
98. Ribas, F.; Doeschate, A.T.; de Swart, H.E.; Ruessink, B.G.; Calvete, D. Observations and Modeling of Surf Zone Transverse Finger Bars at the Gold Coast, Australia. *Ocean Dyn.* **2014**, *64*, 1193–1207. [CrossRef]
99. Almar, R.; Castelle, B.; Ruessink, B.G.; Sénéchal, N.; Bonneton, P.; Marieu, V. High-Frequency Video Observation of Two Nearby Double-Barred Beaches under High-Energy Wave Forcing. *J. Coast. Res.* **2009**, *SI56*, 1706–1710.
100. Grasso, F.; Michallet, H.; Barthélemy, E. Experimental Flume Simulation of Shoreface Nourishements under Storm Conditions. In Proceedings of the Coastal Dynamics 2009, Tokyo, Japan, 7–11 September 2009; World Scientific: Tokyo, Japan, 2009; pp. 1–12.
101. Bouvier, C.; Korteling, J.; Price, T.; Balouin, Y.; Castelle, B. Observation and Modelling of Shoreward Propagating Accretionary Waves (SPAWs) on Microtidal Beaches. *Coast. Eng. Proc.* **2020**, *27*. [CrossRef]
102. Price, T.; van Kuik, N.; de Wit, L.; António, S.; Ruessink, G. Shoreward Propagating Accretionary (SPAWs):Observation from a Multiple Sandbar System. In Proceedings of the Coastal Dynamics 2017 Conference, Helsingør, Denmark, 12–16 June 2017.
103. Mendoza, E.; Jiménez, J.; Mateo, J. A Coastal Storms Intensity Scale for the Catalan Sea (NW Mediterranean). *Nat. Hazards Earth Syst. Sci.* **2011**, *11*, 2453–2462. [CrossRef]
104. Baldock, T.E.; Birrien, F.; Atkinson, A.; Shimamoto, T.; Wu, S.; Callaghan, D.P.; Nielsen, P. Morphological Hysteresis in the Evolution of Beach Profiles under Sequences of Wave Climates—Part 1; Observations. *Coast. Eng.* **2017**, *128*, 92–105. [CrossRef]
105. Baldock, T.; Alsina, J.; Caceres, I.; Vicinanza, D.; Contestabile, P.; Power, H.; Sanchez-Arcilla, A. Large-Scale Experiments on Beach Profile Evolution and Surf and Swash Zone Sediment Transport Induced by Long Waves, Wave Groups and Random Waves. *Coast. Eng.* **2011**, *58*, 214–227. [CrossRef]
106. Birrien, F.; Atkinson, A.; Shimamoto, T.; Baldock, T. Hysteresis in the Evolution of Beach Profile Parameters under Sequences of Wave Climates—Part 2; Modelling. *Coast. Eng.* **2018**, *133*, 13–25. [CrossRef]
107. Dudkowska, A.; Boruń, A.; Malicki, J.; Schönhofer, J.; Gic-Grusza, G. Rip Currents in the Non-Tidal Surf Zone with Sandbars: Numerical Analysis versus Field Measurements. *Oceanologia* **2020**, *62*, 291–308. [CrossRef]
108. Thornton, E.B.; MacMahan, J.; Sallenger, A.H. Rip Currents, Mega-Cusps, and Eroding Dunes. *Mar. Geol.* **2007**, *240*, 151–167. [CrossRef]
109. Castelle, B.; Scott, T.; Brander, R.; Mccarroll, R. Rip Current Types, Circulation and Hazard. *Earth-Sci. Rev.* **2016**, *163*, 1–21. [CrossRef]
110. De Melo Apoluceno, D. Morphodynamique des Plages à Barres en Domaine Méso à Macrotidal: Exemple de La Plage Du Truc Vert, Gironde, France. Ph.D. Thesis, University of Bordeaux, Bordeaux, France, 2003.
111. Houser, C.; Wernette, P.; Trimble, S.; Locknick, S. 11—Rip Currents. In *Sandy Beach Morphodynamics*; Jackson, D.W.T., Short, A.D., Eds.; Elsevier: Amsterdam, The Netherlands, 2020; pp. 255–276, ISBN 978-0-08-102927-5.
112. Castelle, B.; Marieu, V.; Coco, G.; Bonneton, P.; Bruneau, N.; Ruessink, B.G. On the Impact of an Offshore Bathymetric Anomaly on Surf Zone Rip Channels. *J. Geophys. Res. Earth Surf.* **2012**, *117*. [CrossRef]
113. Brander, R.W.; Short, A.D. Morphodynamics of a Large-Scale Rip Current System at Muriwai Beach, New Zealand. *Mar. Geol.* **2000**, *165*, 27–39. [CrossRef]